ADVANCED LECTURES 1985

OPERATIONAL NUMERICAL WEATHER PREDICTION

Lectures 1, 2 and 3

Historical introduction

The global forecasting model

The limited-area fine-mesh model

A J Gadd

Operational Numerical Weather Prediction in the Meteorological Office

1. Historical introduction

After research investigations during the 1950's and early 1960's, numerical weather prediction has been used operationally in the Meteorological Office since 1965. A 3-level quasigeostrophic model was used on the KDF9 computer until 1972, when a 10-level primitive equation model in pressure coordinates was introduced on the 360/195 computer. This 10-level model was used in two forms: for the northern hemisphere north of 15°N with a 300 km grid and for a region near the British Isles with a 100 km grid. The 10-level model was used until 1982. During its lifetime three different integration schemes were used. In 1978 important changes were made in the model's formulation: a more accurate lower boundary condition was introduced and the effects of radiation were included.

In 1982 a 15-level primitive equation model in sigma coordinates was introduced on the Cyber 205 computer. This model is used in two forms: a global version with resolution 1.5° in latitude and 1.875° in longitude, and a fine-mesh regional version with doubled resolution.

This progression of models reflects the scientific advances in numerical weather prediction and the increasing capacity of the computers available. Thus the 15-level model is based on what are currently judged to be the best available treatments of the relevant physics and mathematics, whilst its operational use is made possible by the availability of the powerful Cyber 205 computer.

The design of the 15-level model was based on research that compared alternative techniques. The numerical techniques that had been developed during the lifetime of the 10-level model for the approximation and integration of the governing equations were found to be more efficient than, and equal in accuracy to, the alternatives and so were largely retained. On the other hand the representations of precipitation, convection, turbulence and radiation for the 15-level model were derived from earlier work in the Office on climate research and general circulation modelling. Also inherited from the general circulation work was a mathematical formulation capable of global application and which accommodated the earth's irregular orography. Further improvements in the various components of the model are constantly being researched and are introduced operationally as soon as they are sufficiently proven.

As mentioned above, the 15-level model is used operationally in two versions. There is a global version which is required to fulfil the Office's responsibilities in Defence, as a World Area Forecast Centre for civil aviation, in support of marine and other commercial services worldwide, and to provide guidance for medium range forecasting. The horizontal resolution used is the maximum possible for the original configuration of the Cyber 205 computer, with 1.5° spacing of gridpoints to latitude and 1.875° spacing in longitude. Global forecasts to 6 days ahead are computed twice daily, from 00 GMT and 12 GMT starting conditions and with results available by 05 GMT and 17 GMT, and are distributed to other countries in Europe and elsewhere.

A second, regional, version of the 15-level model has been designed principally to meet the needs of short-range public service forecasting for the United Kingdom and also to support marine services for the European Continental Shelf and the Mediterranean Sea. For these purposes the predictions of precipitation, surface wind and the positions of fronts are crucially important, and these predictions are known to benefit from a closer spacing of the gridpoints. This is achieved within the available computing capacity by using a fine mesh of points (with spacing 0.75° by 0.9375°) over a limited area (80°W-40°E, 30°N-80°N). At the lateral

boundaries of this region the calculations make use of information provided from integrations on the global grid. Forecasts to 36 hours ahead are computed twice daily, with results available by 03 GMT and 15 GMT, and are distributed internationally for use in most of the nations within the region of coverage.

A parallel historical development may be noted in the methods used to provide initial data for the numerical models. The 3-level model required objective analysis of the height field. The 10-level model required objective analysis of the height and humidity fields, but its initial wind fields were diagnosed from the height analysis using the balance and omega equations. The 15-level model uses analysis and data assimilation of potential temperature, surface pressure, humidity mixing ratio and wind component data derived from observations to obtain initial fields of these variables in sigma coordinates. This system has its origins in work carried out as part of the Office's contribution to the Global Weather Experiment in 1979, though very important improvements to the prototype system have been developed in the light of experience.

Associated with both the global and fine-mesh versions of the 15-level model are data assimilation cycles for the analysis of observations to determine the required initial values at the models' gridpoints. The effective quality control of observations and analyses is vital to the success of the forecasts, and here automatic procedures are supplemented by monitoring and intervention carried out by experienced analysts in the Central Forecasting Office. All relevant observations are used, whether derived from land stations, ships, buoys, aircraft or satellites. For the global model the data assimilation is carried out in a 6 hour cycle, taking account of all observations made within 3 hours of each analysis time. For the fine-mesh model the data assimilation is performed in a 3 hour cycle, thus coming close to a continuous assimilation process, with no observation more than $1\frac{1}{2}$ hours from an analysis time.

2. The global forecasting model

a. The model's grid

In the horizontal, the gridpoints of the global model are spaced at intervals of 1.5° in latitude (φ) and 1.875° in longitude (λ). Thus there are 121 x 192 = 23232 points which form the corners of the boxes in the B grid mentioned below. (Of these points, 192 are coincident at the north pole and 192 are coincident at the south pole).

In the vertical, there are 15 levels in sigma ($\sigma = p/p_*$) coordinates. If p_* = 1000 mb the sigma level pressures are

997,975,935,870,790,690,590,490,390,310,250,190,125,66 and 25 mb.

Note the higher vertical resolution near the surface and near 250 mb. The lowest level is about 25 m above the surface.

b. Dynamical and numerical formulation

The primitive equations are used in advective form in sigma coordinates. Finite differences are calculated on a B grid. Wind components (u, v) are held at the centres of grid boxes whilst potential temperature (θ), humidity mixing ratio (q), surface pressure (p_*), vertical velocity ($\dot{\sigma} = D\sigma/Dt$) and geopotential (Φ) are held at the box corners (including the poles).

Thus the independent variables are φ , λ and σ . Among the dependent variables u, v, θ , q and p_* are predicted, and Φ and $\dot{\sigma}$ are diagnosed.

The governing equations are integrated using the split explicit integration scheme. This includes a modified Lax-Wendroff method for horizontal advection and a forward-backward scheme, with trapezoidal integration of the Coriolis terms, for the gravity-inertia adjustment stage.

A time step of 15 minutes is used for the integration of the global model. In order to maintain computational stability, Fourier damping is applied in grid rows near the poles. The damping coefficients in each row, and the equatorward extent of the damping, are determined at the start of each integration as a function of the maximum wind speed and are different in the two hemispheres.

c. Parametrizations

The physical and sub-grid-scale processes represented in the global model at present are as follows.

i. Precipitation, including the ice phase and the evaporation of precipitation as it falls.

ii. Convection, producing a redistribution of heat and moisture in the vertical and based on parcel theory, modified by entrainment, and detrainment.

iii. Surface exchanges and boundary layer turbulence, exchanging heat, moisture and momentum among the four lowest model levels and with the surface.

iv. Radiation, interactive with temperature but assuming climatological humidities and cloud (a fully interactive scheme will be introduced soon).

v. Gravity wave drag, applied at upper levels but calculated from low-level wind and static stability and the variance of orographic height within each grid box.

vi. Horizontal eddy diffusion

vii. Vertical eddy diffusion, at low latitudes only.

d. Surface parameters

The distributions of sea-ice and snow-cover are specified climatologically.

Over open sea, the surface contact temperature is analysed once daily using ship, buoy and satellite observations. The sea surface temperature is held constant during each forecast. Over land and sea-ice the surface contact temperature is predicted using calculated components of the surface energy balance. Specifications are required of albedo, soil moisture and effective thermal capacity.

3. The limited-area fine-mesh model (LFM)

a. Domain and grid

The region of coverage of the LFM is 30-80N, 80W-40E. The grid spacing is 0.75° in latitude and 0.9375° in longitude. Thus the LFM has a doubled horizontal resolution compared with the global model. The same 15 levels are used in both versions.

b. Dynamical and numerical formulation

The LFM has special features as regards measures to maintain computational stability and because of the lateral boundaries. In all other respects the global and fine-mesh models have identical formulations and, indeed, share common coding to a large extent.

A time step of 15 minutes is used for the integration of the LFM. In order to maintain computational stability, multipoint filtering, providing an approximation to Fourier damping, is applied in grid rows poleward of 50N.

c. Parametrizations and surface parameters

In principle, the parametrizations in the LFM are identical to those in the global model. However, it is sometimes necessary or desirable to introduce changes first in one version and later in the other. Current differences are as follows.

i. Convection: the LFM has modifications to prevent spurious showers from shallow convection.

ii. Surface exchanges: the LFM has a modified value of the surface resistance to evaporation.

iii. Radiation: the LFM has an interactive calculation of cloud, and radiation is interactive with temperature, humidity and cloud.

iv. Gravity wave drag is not yet included in the LFM, but will be soon.

d. The LFM approach, its advantages and special problems

The LFM represents the application of the same techniques as used in the global model to regional forecasting with increased horizontal resolution. As such it differs radically from the Meteorological Office's mesoscale model which uses a different dynamical formulation and more detailed treatments of cloud and precipitation.

The increased horizontal resolution of the LFM has advantages in particular for the prediction of precipitation and surface wind. Small-scale systems, especially fronts, and rapid cyclogenesis are better handled.

A number of special problems arise. Some are associated with the increased resolution, but the most troublesome arise in connection with the lateral boundary conditions.

e. Lateral boundary conditions

The advantages available through improved horizontal resolution in LFMs are contingent upon an adequate method for updating the lateral boundaries during the course of the forecasts. Theoretical investigation of this problem for the primitive equations has proved to be rather intractable. Guided by

analogies with theoretical results for quasigeostrophic formulations, several investigations have been made where the normal component of velocity at the boundary is specified externally, say from a global model, whilst other predicted variables are specified at inflow points but determined internally at outflow points. Such methods have worked well in particular cases, but, for the wide generality of circumstances encountered in operational prediction, methods which allow complete overspecification (ie all predicted variables are externally specified at all boundary points) have proved more reliable.

Three alternative methods are available which allow complete overspecification of the boundaries. Two of these involve the use of externally specified tendencies at boundary points. In one scheme (used in the Meteorological Office) enhanced diffusive damping is applied in a boundary zone, whilst in the second prescribed tendencies are used in the boundary zone also, and are given a weight which falls to zero as one moves to the interior region. In the third scheme the predicted variables in the boundary zone are relaxed towards prescribed values on a time scale that increases as one moves toward the interior region.

Whilst each of these pragmatic methods has been used successfully in limited area modelling, theoretical analysis with simplified equations has highlighted potential shortcomings of all three. For the diffusive damping approach the boundary zone should be as narrow as possible to reduce the transit time, and thus the overall damping, of incoming meteorological features. For the weighted tendencies scheme and the relaxation scheme the boundary zone must be fairly wide, allowing gradual changes in the weights or the relaxation coefficients, to avoid reflection of outgoing waves. A fourth pragmatic method, known as the pseudo-radiation scheme, seemed at first to offer possible advantages, but this promise has not been fulfilled.

ADVANCED LECTURES 1985

OPERATIONAL NUMERICAL WEATHER PREDICTION

Lecture 4

Analysis and assimilation

M. J. Atkins

OPERATIONAL NUMERICAL WEATHER PREDICTION

Analysis and Assimilation

Margaret J Atkins

1. Introduction

A necessary condition for a numerical model of the atmosphere to produce a good forecast is that the initial values of the model variables should be well specified. They should properly represent all the features, which can be resolved by the model, present in the atmosphere on a given occasion, and they should not contain imbalances between the variables which would excite spurious oscillations in the subsequent forecast.

Nowadays observations are received which may be valid at any time during a 24-hour period. The maximum number of conventional observations are still received for 00 and 12 GMT, this being the time at which most upper-air observations are made. For this reason forecasts still start from an analysis valid at those times. However, significant numbers of both surface and upper-air observations are received for 06 and 18 GMT and reports valid at any time are received from satellites, aircraft and drifting buoys. Data assimilation schemes are designed to make the best use of all this information, in particular, to use information valid at all times of the day to produce the best possible analysis valid at 00 or 12 GMT from which to start a forecast.

At the Meteorological Office, this is achieved by producing a global analysis at 6-hourly intervals, 00, 06, 12 and 18 GMT. All observations valid within three hours of each of those times are used to modify a six-hour forecast starting from the previous analysis. Information from observations valid at all previous times is thus carried forward to the

current analysis in a process analogous to the use of continuity charts in subjective analysis. The prognostic variables of the forecast model are potential temperature (θ), westerly and southerly wind components (u,v), humidity mixing ratio (q) and surface pressure (p^*), which are carried on a latitude/longitude grid in the horizontal and 15 levels in the vertical defined in terms of terrain-following sigma coordinates (as described by Dr Gadd in the previous lectures). The analysis is performed directly in the model variables on a grid identical to that of the forecast model except that the number of points per latitude circle decreases polewards of 50° to maintain a quasi-uniform spacing. Observations must therefore first be processed (to be described in the subsequent lecture by Dr Woodage) to provide data in terms of the model variables, but not necessarily at model sigma levels.

2. Quality Control

Univariate, three-dimensional statistical interpolation (sometimes known as optimum interpolation) is used in the analysis to interpolate from the observation points to the grid points. However, before this process is carried out, observations are subjected to quality control making use of the same technique. As a first step the observations are checked against the six-hour forecast from the previous analysis, and when the difference exceeds a criterion dependent on the characteristic error of both the observations and the forecast, the observation is flagged. In the second step, each observation (including those that have been flagged) is checked by comparing it with a value interpolated from the surrounding unflagged observations, again using statistical interpolation. If the difference exceeds a second criterion, which depends on the characteristic error of the observation and the interpolation error (which may be determined from

the method of statistical interpolation), the observation is rejected. Observations which fail the first check may be reinstated if they pass the second check, ie observtaions which differ significantly from the six-hour forecast field may be retained if they are supported by other observations.

3. Statistical interpolation

Observations which pass the quality control checks (including those performed within the Synoptic Data Bank and the manual monitoring of the Central Forecasting Office), are used to interpolate values of each of the model variables at the analysis grid points. Interpolation is actually carried out in terms of the departure of an observation from the model field to give an increment or correction to the model field at each of the grid points, according to equation (1).

$$\Delta\psi_g = \sum_{i=1}^{Nobs} w_i \left(\psi_i^{obs} - \psi_i^{model} \right) \qquad (1)$$

where ψ_i^{obs} is an observation of one of the model variables θ, u, v, q, p^*.

ψ_i^{model} is the model value of the same variable interpolated to the observation point.

$\Delta\psi g$ is the correction or observational increment for the variable ψ at the grid point,

and w_i is the weight given to observation ψ_i^{obs}.

The summation is taken over a maximum of seven observations of the given variable surrounding the grid point in three dimensions. The weights w_i are determined by minimizing the interpolation error over a large number of cases. They may then be expressed as a function of the pre-specified characteristic errors of the observations and model field, and the

3-dimensional spatial distribution of the observations around the grid point. The displacement time of the observation from the analysis may be taken into account by modifying the observational error.

4. Assimilation

In the most common method of applying statistical interpolation, the model field used is the six-hour forecast and the whole of the correction $\Delta\psi_g$ is added to this field to produce the analysis. The technique is usually applied in a more sophisticated form than that described above so that, for example, observations of wind may affect a height analysis, and vice versa, through the geostrophic relationship. However, even when such a sophisticated multivariate scheme is used, the simple correction of a six-hour forecast by an interpoalted increment will excite spurious high-frequency oscillations in a subsequent forecast. These oscillations are caused by small errors in the analysis which result in imbalances between the mass and wind field and unrealistic values of the divergent component of the wind. They produce a noisy forecast and, more seriously, dissipate much of the information from the observations present in the analysis. The usual technique for overcoming this problem is to apply some kind of initialization. The grid-point values of the model variables are adjusted to satisfy certain mathematical constraints which remove the high-frequency oscillations while at the same time ensuring that values remain close to the observations. The most popular form used today is non-linear normal mode initialization.

At the Meteorological Office an alternative approach is used. The observations are assimilated into the model during the six-hour forecast preceding the analysis time. First the interpolation weights w_i are calculated using values of the model forecast error appropriate to a

six-hour forecast. Then at each time-step of the six-hour forecast preceding the analysis, increments are calculated at each of the grid points from differences between the observations and the current model state using the pre-determined weights, by means of equation (1). However, only a small proportion (λ) of these increments is added to the model field. This process is represented in equations (2) to (4). Let one timestep of the model be represented by equation (2)

$$\underline{\psi}^{*}_{t+\Delta t} = \underline{\underline{M}}\,(\underline{\psi}_{t}) \qquad (2)$$

where $\underline{\psi}$ is now a vector representing all the model variables and $\underline{\underline{M}}$ is an operator representing one timestep of the model. $\underline{\psi}^{*}_{t+\Delta t}$ is the value of the forecast without assimilating any data. It is then modified by the observations according to equation (3).

$$\underline{\psi}_{t+\Delta t} = \underline{\psi}^{*}_{t+\Delta t} + \lambda\, \Delta\underline{\psi}_{t+\Delta t} \qquad (3)$$

where $\Delta\underline{\psi}_{t+\Delta t}$ is a vector representing increments at the grid-points interpolated from the observations for all variables at time $t+\Delta t$. For any variable, ψ, at a grid point

$$\Delta\psi_{t+\Delta t} = \sum_{i=1}^{N_{obs}} w_i \left[\psi_i^{obs} - \psi^{*}_{i\ t+\Delta t} \right] \qquad (4)$$

Equation (4) is the same as equation (1) with a slight change of notation. λ increases linearly from 0 to 0.125 during the six-hour period, so that only small changes are made to the forecast fields. This process is illustrated schematically in Figure 1. Additional damping is included in the forecast model to control any unwanted oscillations which are generated. Since the interpolation is purely univariate changes to the surface pressure and temperature fields do not directly affect the winds

and changes to the surface pressure field do not directly affect the temperature structure aloft. To assist the assimilation of the data, additional geostrophic wind increments are calculated from the surface pressure and potential temperature increments, and added to the wind field at each timestep; also, additional potential temperature increments are calculated from the surface pressure increments using the hydrostatic equation, and added to the potential temperature field at each timestep.

The "assimilation cycle" for the global model may be summarized as follows. Observations valid within three hours of 06 GMT are assimilated into the six-hour forecast starting at 00 GMT and the resulting field is the 06 GMT analysis. Observations valid within three hours of 12 GMT are then assimilated into the six-hour forecast starting from this 06 GMT analysis. The process continues in a similar way for the remainder of the 24-hour period. In practice the situation is a little more complicated as forecasts have to be run as early as possible in order to be useful. At present, therefore, the 00 and 12 GMT assimilations are actually performed twice, once to start the global model forecast at 0320/1520 GMT and once as part of the assimilation cycle at about 1130/2230 GMT. This repeat or "update" assimilation is run as late as possible to allow time for extra data to be received and for CFO to carry out intervention. The update assimilation is followed immediately by the 06 or 18 GMT assimilation.

5. Fine-mesh assimilation

Initial fields for the regional fine-mesh model are provided by a fine-mesh assimilation. This is based on the same principle as the global assimilation except that the assimilation is performed by the regional model, at three-hourly intervals instead of six and, for each assimilation, observations within $1\frac{1}{2}$ hours of the analysis time are used. Global

information from observations made at earlier times is incorporated by restarting every 12 hours by interpolation from a global update assimilation and performing 12 hours of fine-mesh assimilation at 3-hourly intervals to provide an initial field for the fine-mesh model valid at 00 or 12 GMT. Lateral boundary conditions for this fine-mesh assimilation are provided by a 12-hour coarse-mesh forecast from the global update assimilation. The fine-mesh assimilation scheme has therefore both a higher spatial and temporal resolution than the global assimilation and this enables more detailed analyses to be made.

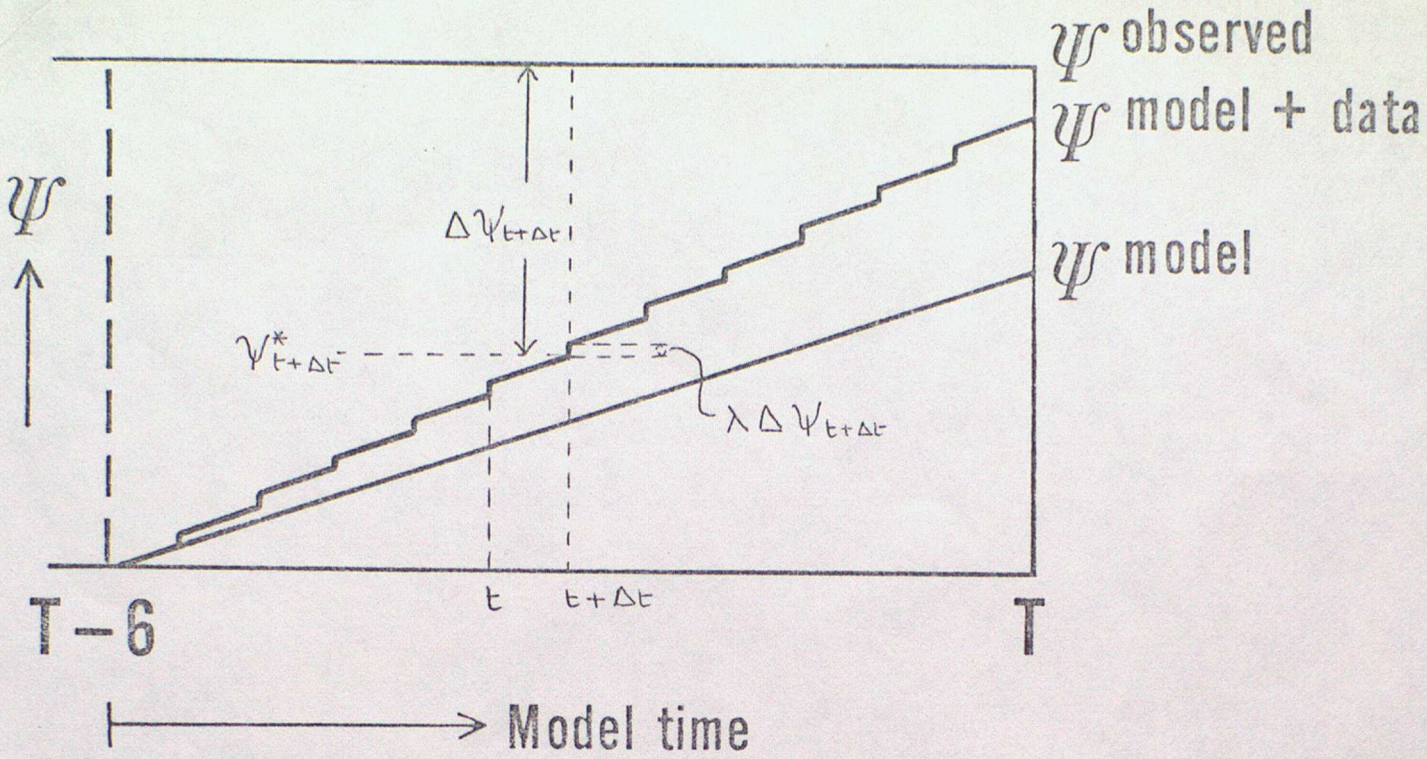

Figure 1. Schematic Diagram of Data Assimilation

The vertical co-ordinate ψ represents the state of the model or the atmosphere. The horizontal co-ordinate is the model time in hours. T is the validity time of the assimilation depicted and T-6 is the time of the previous assimilation. $\psi^{observed}$ is the state of the atmosphere as determine from observations at time T. ψ^{model} is the 6-hour forecast from the previous assimilation at time T-6. $\psi^{model+data}$ is the result of assimilating observations for time T into the 6-hour forecast from T-6. t and t+Δt are two successive timesteps of the forecast and $\psi^*_{t+\Delta t}$, $\Delta\psi_{t+\Delta t}$ and λ are as defined in the text. Note that $\psi^{model+data}$ will not equal $\psi^{observed}$ as allowance is made for errors in the observations.

ADVANCED LECTURES 1985
OPERATIONAL NUMERICAL WEATHER PREDICTION

Lecture 5

Observations and intervention

M.J.Woodage

List of Symbols

p	Pressure (mb)
PMSL	Pressure at mean sea level
Ps	Pressure at station level (surface)
p*	Pressure at model surface
T	Temperature (K)
Tv	Virtual (dry air) temperature (K)
T_d	Dew point temperature
PWC	Precipitation water content (mm)
R.H.	Relative humidity
q	Humidity mixing ratio (gm/gm)
z	Geopotential height
$\underline{V}$	Wind vector
u,v,	Eastward and Northward wind components
θ	Potential temperature

OBSERVATIONS AND INTERVENTION

1. Introduction

Coded observational data arrive at Bracknell via the Global Telecommunications System (GTS) and are routed by Met O 5 (Telecommunications) to Met O 12 (Data Processing), where the data are decoded and stored on the IBM computer in the Synoptic Data Bank. Data are stored in their original form, but on retrieval some basic quality control is performed (eg radiosonde ascents are checked for internal consistency) and any data suspected of being in error are flagged. Forecasters are able to call up flagged or unflagged data on Visual Display Units in the Central Forecasting Office (CFO) and submit any rejections or corrections considered necessary. In addition to the quality control carried out in the data bank, several terminal programs are available which compare the data against the model 'first-guess' or 'background' field (a forecast from the previous analysis verifying at the appropriate data-time). Data which differ greatly from the first guess field are displayed for inspection and possible correction or rejection by the forecasters. In addition to monitoring the observational data, forecasters are also able to enter 'bogus'or 'invented' observations in areas where the model fields are poor. These can be values of height, temperature, wind, humidity, or mean sea level pressure. At the beginning of a forecast sequence, the data are extracted from the data bank, amended in accordance with the intervention, and passed across to the Cyber computer. The data are then processed into a form acceptable to the analysis program. This involves converting all observed variables to analysis variables, and sorting the observations into latitude order. The conversion of some types of data is quite straightforward, but others pose more problems, and are described in the second section. In the third section a brief description is given of the intervention facilities available in CFO.

Figure 1 is a flow chart of the processes described above.

2. Observational data

Figure 2 shows the observational variables available and the corresponding analysis variables derived from them. The conversion methods are outlined below.

Surface Data (SYNOPS)

The equation for calculating p* (pressure at model topography z*) from p_r (reported pressure, either at mean sea level or station level z_r) is obtained by integrating the hydrostatic equation over the layer assuming a temperature structure with constant lapse rate of 0.0065°K per m. Reported temperature is not used in the calculation as it is subject to boundary layer effects. Instead, a model 'surface' temperature T* is constructed by extrapolating from a sigma level outside the model boundary layer (again assuming constant lapse rate). This method has the advantage of being the direct inverse of the calculation used to convert p* to mean sea level pressure for model output.

Figure 3 shows the equations used.

Upper Air data (TEMPS, PILOTS)

A typical radiosonde ascent contains more levels of data than can be handled by the analysis and more vertical detail than can be resolved by the model. Therefore, at the conversion stage, the full ascent is condensed to provide representative data at sigma levels only. The simplest method of achieving this is by interpolating linearly in ln(p) from the nearest two adjacent reported levels. However, this method can result in unrepresentative values being passed to the analysis if a model sigma level happens to lie close to an extreme value in the observed ascent(eg the tropopause). To overcome this, sigma level data are calculated as a weighted mean of all reported values in the layer centred on the sigma level. This generally results in a smoothing of the data, but gives a better representation of the ascent on the scale of the model grid.

Figure 4 gives details of the method.

The radiosonde systematic height corrections (Hawson corrections) are incorporated into the data as equivalent temperature corrections which are applied at each sigma level.

Satellite temperature soundings (SATEMS)

Three types of SATEM data are currently available: the conventional and high resolution data received via the GTS, and the locally processed 'HERMES' data.

The conventional SATEMS are received in the form of thicknesses between standard levels, and for clear soundings, layer precipitable water content values. Thicknesses are converted to virtual temperatures at midpoints of standard levels, and precipitable water content values used to correct these to actual temperatures. For cloudy soundings, a constant relative humidity (80%) is assumed to calculate corrections. The high resolution SATEMS are treated in a similar way (omitting the first step), with the reported virtual temperatures being assigned to the midpoints of the standard layers. (Note that these are not yet used in the operational analysis).

The HERMES data are available directly in the form of (true) temperatures at standard levels, and only require conversion to potential temperatures.

Satellite cloud-track winds (SATOBS)

The wind data are simply passed to the analysis at the pressure levels specified in the report.

Aircraft data (AIREPS)

Flight levels are converted to pressure levels using equations based on the ICAO Standard Atmosphere. Temperatures are then converted to potential temperatures, and passed with the wind data directly to the analysis at the appropriate pressure level.

PAOB data

These are artificial observations generated by Australian forecasters to force their model initial fields to fit their manual analyses. They are broadcast on the GTS but arrive too late for the main forecast run; however they are used in the update analysis with a very low weight, and are pre-processed in a similar way to the BOGUS height data generated by CFO (discussed in the next section).

3. Intervention facilities

With the exception of Upper Air (radiosonde) data, all observations can be displayed individually or by area block with equivalent model field values for comparison. The following action may then be taken by forecasters:

SYNOPS

Observations from individual stations or ships may be rejected. Currently the entire report must be removed, but the facility to reject or correct separate elements of a report is to be introduced. For drifting buoys, blocks of data within a specified area may be rejected.

TEMPS AND PILOTS

Observations from individual stations or ships may be rejected (at present the entire report must be rejected). Reported heights and temperatures may be changed in a standard way by correcting the 100 mb height (effectively altering the Hawson correction), and reports from the UK area may be corrected by re-taping the message in Met O 5 (COR message). It is intended to introduce facilities to reject or correct separate elements of radiosonde reports, using graphics devices to display the many levels of data in a compact form.

SATEMS

Individual soundings may be rejected, either completely or at specified levels. Blocks of soundings within a specified area or time band may also be rejected.

SATOBS

Individual observations, and blocks of observations within a specified area or time band may be rejected.

AIREPS

Individual reports may be rejected, and also blocks of reports within a specified area, time band or range of vertical levels. The facility to reject temperature and wind data separately is to be introduced.

PAOBS

Individual reports and blocks within a given area may be rejected. There is a permanent rejection area over the South Atlantic.

BOGUS data

Bogus values of wind, humidity and temperature are passed to the analysis at the pressure levels specified, and mean sea level pressures are converted to p* values using the same method as for SYNOP data. Bogus heights are more difficult to deal with, as they must be converted to temperatures; for this reason, heights may only be entered at certain standard levels, namely 850 mb, 500 mb, 250 mb, 100 mb or 50 mb. A model height field is used to calculate the height changes at the intervention levels implied by the bogus data; thickness changes between the intervention levels are then derived, and converted to layer mean temperature increments. A temperature profile is then constructed fromthe model standard level heights and each temperature incremented by the appropriate change for the layer. The method is illustrated in Fig 5. A facility exists in CFO to display temperature profiles derived from bogus height data in tephigram form on a graphics device.

Figure 1 Flow-chart showing the different steps involved in preparing the data for the analysis.

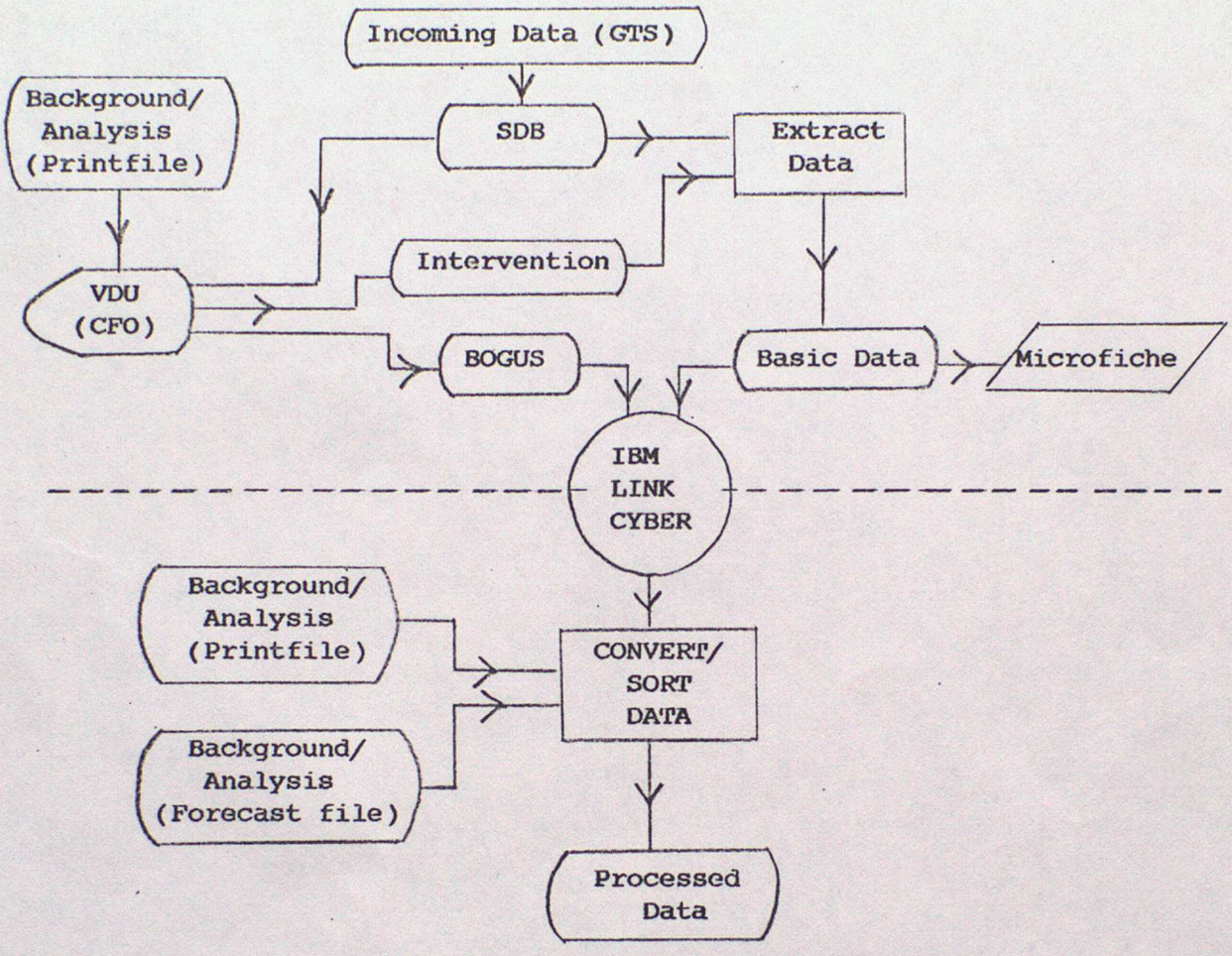

Figure 2 Variables received from each observation type and analysis variables derived from them.

TYPE	BASIC DATA		PROCESSED DATA	
	VARIABLES	LEVELS	VARIABLES	LEVELS
Surface Land	PMSL or ps, $T, T_d, \underline{V}$	MSL, surface	p^*	Model Surface
Surface Ship	PMSL, $T, T_d, \underline{V}$	MSL	$p^*, q, \underline{V}$	Model Surface
Drifting Buoy	PMSL	MSL	p^*	Model Surface
Upper Air TEMP	$ps, Z, T, T_d, \underline{V}$	Standard Significant	$p^*, \theta, q, \underline{V}$	Sigma
Upper Air PILOT	$\underline{V}$	Standard Significant	$\underline{V}$	Sigma
SATEMS: Conventional High Resolution HERMES	 Thickness, PWC Tv, PWC T, PWC	 Standard Standard layers Standard	 θ θ θ	 Sigma Sigma Sigma
SATOB	$\underline{V}$	As reported	$\underline{V}$	As reported
AIREP	$T, \underline{V}$	As reported	$\theta, \underline{V}$	As reported
BOGUS	Z PMSL, $T, \underline{V}$, R.H	Intervention As reported	θ $p^*, \theta, \underline{V}, q$	Mid-pts Standard As reported
PAOB	PMSL, thickness	MSL, 500 mb	p^*, θ	Mid-pts Standard

Figure 3 Calculation of p*

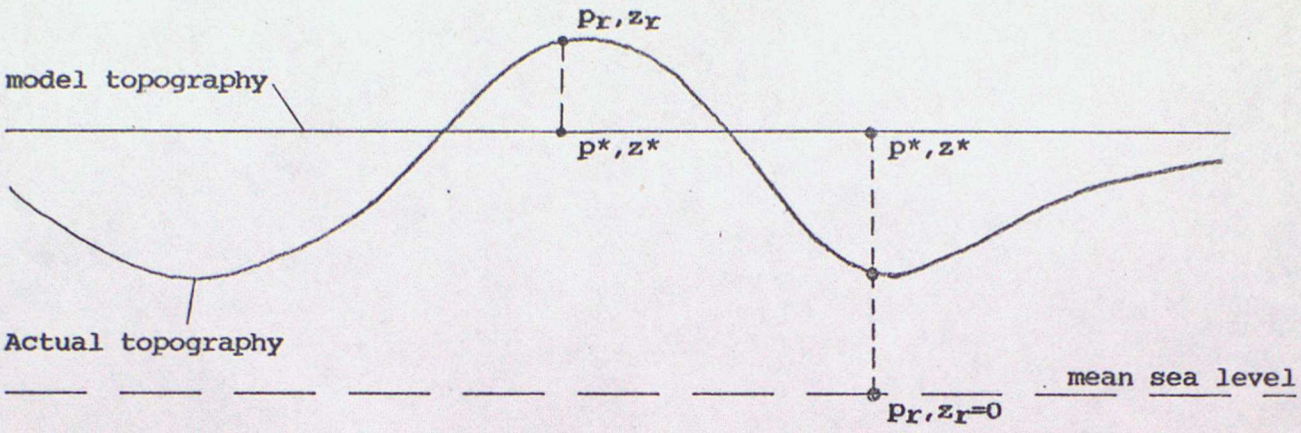

Integrating the hydrostatic equation over a layer (p_1, p_2), (Z_1, Z_2):

$$\int_{p_1}^{p_2} \frac{1}{p}\, dp = \frac{-g}{R} \int_{Z_1}^{Z_2} \frac{1}{T}\, dz$$

where $g = 9.80665$, $R = 287.05$ J kg^{-1} k^{-1}

Assuming $T(Z) = T_o - \gamma\,(Z-Z_o)$ gives

$$\ln \frac{p_2}{p_1} = \frac{g}{\gamma R} \ln \left[\frac{T_o-\gamma(Z_2-Z_o)}{T_o-\gamma(Z_1-Z_o)}\right]$$

Then $$\frac{p_2}{p_1} = \left[\frac{T_o-\gamma(Z_2-Z_o)}{T_o-\gamma(Z_1-Z_o)}\right]^{\frac{g}{\gamma R}} = \left[\frac{T(Z_2)}{T(Z_1)}\right]^{\frac{g}{\gamma R}}$$

This result is used to obtain a model surface temperature T* from the fifth σ -level temperature T_5:

$$T^* = T_5 \left(\frac{1}{\sigma_5}\right)^{\frac{\gamma R}{g}}$$

and the model surface pressure p* from the reported p_r:

$$p^* = p_r \left[\frac{T^*}{T^*-\gamma(Z_r-Z^*)}\right]^{\frac{g}{\gamma R}}$$

Figure 4 Calculation of sigma level data from radiosonde ascents

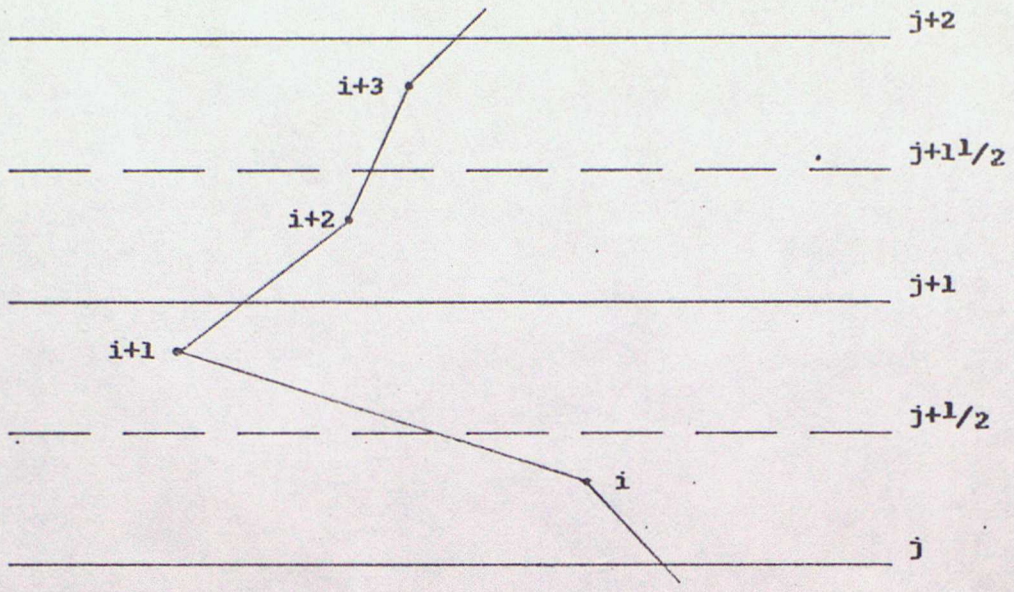

Given an ascent with reported levels i, data (eg temperature T) at σ -levels j are calculated as follows:

First interpolate to the sigma half levels which bound the layer centred on the σ -level:

$$T_{j+1/2} = T_i + \left(\frac{T_{i+1} - T_i}{\ln \frac{p_{i+1}}{p_i}}\right) \ln \frac{p_{j+1/2}}{p_i}$$

$$T_{j+1 1/2} = T_{i+2} + \left(\frac{T_{i+3} - T_{i+2}}{\ln \frac{p_{i+3}}{p_{i+2}}}\right) \ln \frac{p_{j+1 1/2}}{p_{i+2}}$$

Then form the weighted mean of all observed data in the layer:

$$T_{j+1} = \left[(T_{j+1/2} + T_{i+1}) \ln \frac{p_{i+1}}{p_{j+1/2}} + (T_{i+1} + T_{i+2}) \ln \frac{p_{i+2}}{p_{i+1}} \right.$$

$$\left. + (T_{i+2} + T_{j+1 1/2}) \ln \frac{p_{j+1 1/2}}{p_{i+2}} \right] \; 2 \ln \frac{p_{j+1 1/2}}{p_{j+1/2}}$$

Figure 5 Conversion of BOGUS heights to temperatures

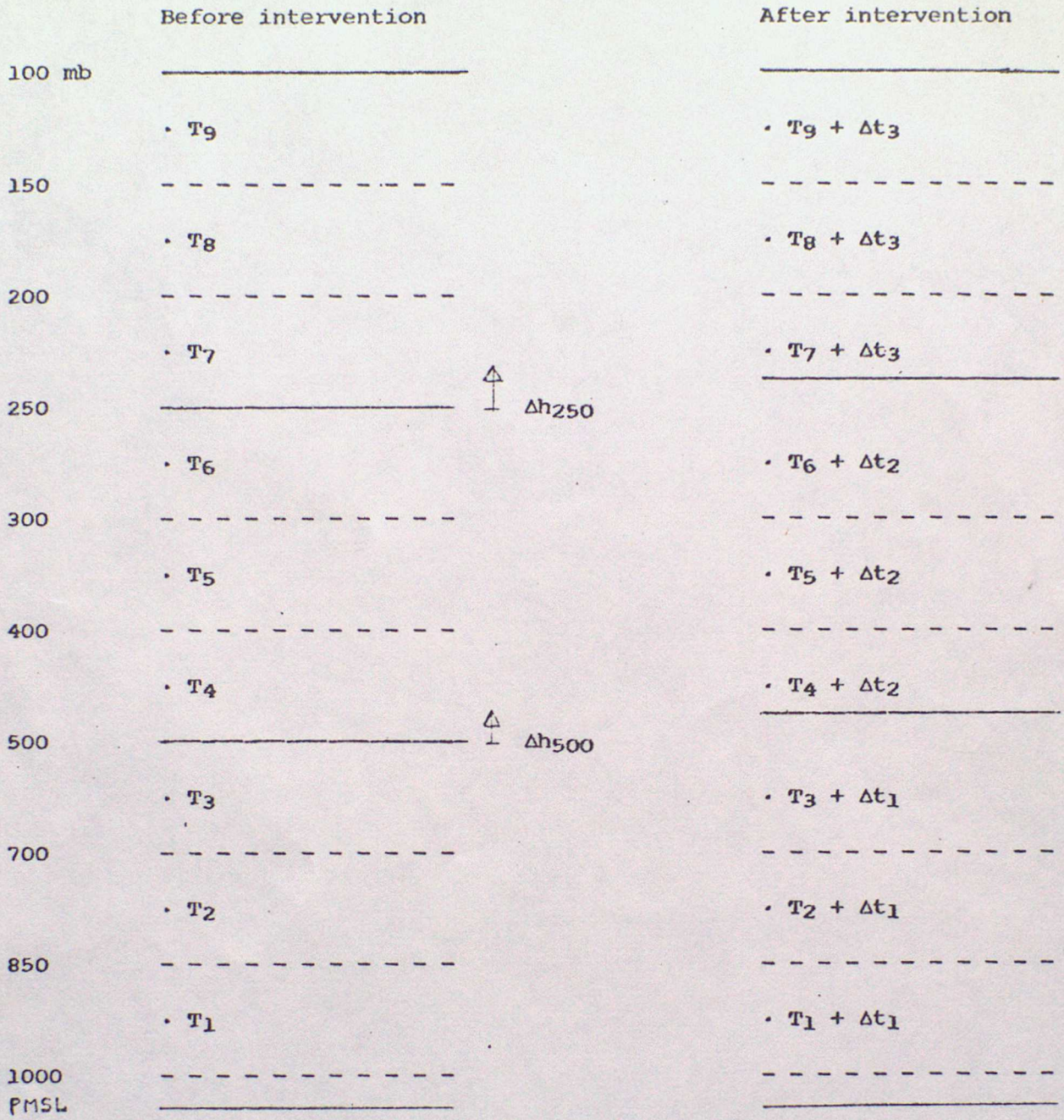

Model temperatures T are obtained from the standard level heights using the hydrostatic equation integrated assuming constant tempterature, eg

$$T_1 = \frac{g}{R} \left(\frac{h_{850} - h_{1000}}{\ln \frac{1000}{850}} \right)$$

Temperature increments are calculated similarly, eg

$$\Delta t_2 = \frac{g}{R} \left(\frac{\Delta h_{250} - \Delta h_{500}}{\ln \frac{500}{250}} \right)$$

where $\Delta h_{500} = h_{500}(\text{bogus}) - h_{500}(\text{model})$

ADVANCED LECTURES 1985

OPERATIONAL NUMERICAL WEATHER PREDICTION

Lectures 6 and 7

Post-processing of results

Output products

C J Devrell and P E Francis

Summary

The data produced by the numerical weather prediction models are further processed in order that a comprehensive set of output products can be generated operationally. The first step is the generation of an output data set which contains both primary and derived variables, arranged on fields at constant standard pressure levels. The derived variables are those which are not explicitly contained in the forecast model data.

Charts and coded bulletins are then constructed from the output data set, using a variety of formats requested by users, and internationally agreed. Lists are provided of the current charts and code bulletins available. A discussion of back-up arrangements concludes the presentation of output products.

1. Introduction

The NWP models described in earlier lectures yield large amounts of data when run operationally. These data (for different variables, model gridpoints, model levels, forecast times) are internally arranged and represented in a form that is convenient for the rapid

integration of a numerical model. Such a representation is however far from convenient for the production of the large quantity of output, in many forms, that is needed to satisfy the requirements of modern meteorological services. In order that a versatile range of output products can be easily generated it is first necessary to re-arrange the forecast model data fields into a more suitable format. At the same time it is convenient to generate (by further modelling techniques) those fields which are not explicitly carried in the models, but which are required for operational purposes. These 'derived' fields are listed in Table 1, together with the other standard formats for explicitly held variables.

The output variables, held in a comprehensive data set, are then transferred from the Cyber 205 fast vector processor to a conventional 'front end' processor, currently either an IBM 3081 or IBM 370/158. The latter processor is due for replacement during 1985, the new machine being specified as having to carry the full load of output processing while working on its own. After reformatting, the output data set is available for access by authorised users, as well as being the source of all the operational output data streams. A versatile suite of access routines is available which allow data to be extracted and then interpolated onto a wide range of latitude-longitude grids, and also onto different map projections, including Polar Stereographic and Mercator. Another advantage of retaining output products on a front end processor is the ease of communication with other computing systems, and the fact that incoming back-up data from the National Meteorological Center (NMC) in Washington

DC, and medium range data from The European Centre for Medium Range Weather Forecasts (ECMWF), can be collected and stored in the same output format, ready for presentation in chart form using standard computer software.

Table 1

Variables stored in output formats, both basic and derived

Model Variable	Basic output forms	Derived output forms
Wind	Speed and direction on standard pressure levels	Vertical velocity at standard levels. Maximum wind, height, speed, direction. Surface (10 m) wind, speed, direction. Vorticity at standard levels. Clear air turbulence index (200, 250, 300 mb).
Temperature Surface pressure	Temperatures and heights of standard pressure levels. Mean sea level pressure	Tropopause temperature, pressure, height. Height and pressure of freezing level. Surface (1.5 m) temperature. Wet bulb potential temperature (500, 850 mb)
Humidity	Relative humidity at standard pressure levels $\geq$ 500 mb.	
Precipitation	Dynamic and convective rates and accumulations.	

2. Output modelling techniques

The first stage in the process of generating output products (Fig 1) is the construction of a comprehensive data set which consists of the required basic and derived variables, stored on pressure levels. Table 1 briefly sets out the current contents of the output data set. Not all of the derived fields are generated by both versions of the NWP model (ie

global and fine mesh versions), but all of the basic output forms are common to both. Variables directly associated with aviation forecasting (tropopause and maximum wind for instance) are only generated from global model data.

(a) Wind modelling

The initial step in the wind modelling is the calculation of the vertical velocity. This calculation is performed while the horizontal wind components are still on σ-levels, and is carried out in a manner similar to that employed in the forecast model. Divergences at every gridpoint are calculated for each model layer, and summed from the top downwards. In the same manner absolute vorticity is also calculated from the horizontal wind components, before interpolation onto pressure levels is carried out. The required interpolation, for both vertical velocity and absolute vorticity, is calculated by assuming that the variables change linearly with the logarithm of pressure, written log(pressure) below.

The next step is to calculate the speed, direction and pressure level of the maximum wind. The wind components are first combined to give a speed and direction, then a search is made for the σ-level that contains the maximum value of wind speed. The maximum of the implied continuous profile may then be assumed to lie within one model layer on either side of the designated σ-level. A cubic spline function is fitted to the wind speed values outside of the boundary layer, and by means of straightforward but detailed calculus and

algebra it is possible to calculate both the profile maximum value and its level. An enhancement of the maximum value is not presently thought to be necessary since the improved definition of jet streams in the present model gives acceptable results in most situations. The direction of the maximum wind is found by means of interpolation in log(pressure) once the level has been determined.

Consistent with the vertical interpolation used for other wind parameters, wind speed and direction on standard levels are determined by assuming a linear variation with log (pressure) between the σ-levels. The maximum wind information is used as an extra level in order to give consistency in that region. Standard levels that fall below model orography are assigned the wind speed and direction of the lowest σ-level.

Another derived 'wind' parameter is the clear air turbulence (CAT) index, which is calculated using the formulation established for the previous NWP model (Dutton, 1980). Work on updating the formulation, using data from the new NWP model related to aircraft reports of CAT, is now under way, and should lead to improvements in the definition of this very important aviation index.

Finally in this section on wind modelling, we turn to the problem of calculating a surface wind defined as the wind at 10 m above the ground/sea surface. For many forecasting applications such a wind parameter is an essential element and it is important that realistic values are derived. The technique used during the output

modelling calculations is consistent with that employed in the forecast model for representing boundary layer effects. An integral part of the system is the calculation of a boundary layer Richardson number, taken to be a function of wind, temperature and humidity values at the surface and lowest σ-levels. This Richardson number then determines the profiles used to evaluate both surface wind and temperature over land and over sea. The profiles vary with the implied stability in the boundary layer, and contain the implicit contributions of surface roughness length and drag coefficient. The direction of the surface wind is taken to be that of the wind in the lowest σ-level.

(b) Temperature modelling

The first stage in the process of calculating the heights and temperatures of standard levels is to convert the potential temperatures on σ-levels, used in the forecast model, into the associated temperature values. Then the thickness between σ-levels can be calculated using the σ-level virtual temperatures. In this way the effects of humidity on the thicknesses are included. The heights of the σ-levels can then be derived by summation of thicknesses from the lowest level upward. The temperature at each standard pressure level is calculated firstly by locating it between two σ-levels, and then by assuming a constant temperature lapse rate between those levels . The height at each standard pressure level is calculated by

assuming a constant virtual temperature for the layer between the pressure level and the lower (in height) of the two reference σ-levels.

For pressure levels below the model orography it is necessary to adopt a pragmatic approach in order to obtain acceptable temperature and height values. The associated calculation of pressure at mean sea level is performed in a consistent manner. Height values below orography are primarily required so that realistic contour charts can be produced for the forecaster. Such charts require to be smooth, and to appear as if the intruding orographic feature was not present. Accordingly it is acceptable to extrapolate from a 'free atmosphere' level in order to obtain the temperature for a subterranean standard level, thus avoiding the effects of the boundary layer. The extrapolation uses a standard lapse rate of $0.0065°K\ m^{-1}$. The height at the subterranean standard level is obtained by subtracting the thickness of the layer between the lowest σ-level and the standard pressure level concerned, again calculated using the assumption of a constant virtual temperature throughout the layer. The pressure at mean sea level is given by an equivalent calculation using the orographic height and an extrapolated temperature profile as above. For zero orography the pressure at mean sea level is of course equal to the surface pressure.

The next task is to locate the tropopause and assign a consistent temperature and height. The essence of the method employed to do this is the assumption that the tropopause should be associated

with a layer mean lapse rate of less than 0.002°K m^{-1}, at a height above that of surface inversions and other low level temperature features. Layer mean lapse rates are therefore calculated, from the σ-level data, and a search is carried out (above 500 mb) for the relevant critical lapse rate. Having found the first layer for which the mean lapse rate is less than the critical value it is a straightforward algebraic task to calculate the exact σ-level for which the lapse rate equals 0.002°K m^{-1}, assuming a linear variation in the lapse rate between the mid points of adjacent layers. Following further algebraic manipulation the temperature of the tropopause can be determined, and then in the same manner as described earlier the height can be calculated.

Three other temperature dependent variables are also derived. The freezing level is located by searching upward through the σ-level data for the first value of temperature less than 273°K. The freezing level height and temperature are then calculated by assuming a constant lapse rate through the appropriate model layer. The technique for modelling surface parameters was outlined earlier in the discussion of wind variables. By this method a temperature at 1.5 m is modelled and made available for output. Finally, values of wet bulb potential temperature are calculated by an iterative technique after the necessary temperature and humidity information has been transferred onto pressure levels.

(c) Humidity and rainfall

The forecast model produces values of humidity mixing ratio on σ-levels whereas for output purposes relative humidity on pressure levels is required. The first step in the transformation process is the calculation of saturation mixing ratio, performed by using a look-up table for saturation vapour pressure with reference to the σ-level temperature. The look-up table assumes saturation with respect to water for temperatures greater than -5°C, and with respect to ice for temperatures less than -10°C. For intermediate values the table has an interpolated entry between the two saturation states. The information is then at hand to be able to first calculate saturation mixing ratio and then relative humidity. Interpolation to pressure surfaces is again achieved by assuming a linear variation in log(pressure).

Rainfall information in the models is available both as the result of convective and dynamic processes, the basic parameter being an instantaneous rate. By accumulating the rates at each time step and multiplying by the appropriate constant it is also possible to derive values for dynamic and convective accumulations over a period. This calculation is performed in the forecast model. Enhancement of the gridpoint convective values in order to represent possible convective activity in a fraction of a grid square is at present performed empirically; but the use of relevant information from the convective parametrization in the forecast model may lead to a more satiafactory procedure for such enhancement.

3. Chart output

The conventional presentation of most forecast products is by means of a chart, either containing isopleths of the required field or having numerical values printed on a regular grid. Chart products form a very important part of the output stream from the numerical models run at Bracknell. Including all kinds of charts, and those required for back-up purposes, nearly 1000 are produced in a 24 hour cycle. Not all of these are transmitted by facsimile broadcasts of course. Nearly half of them are for back-up purposes, ie for use if a later forecast run fails. Many are for use in the Central Forecasting Office and are not designed for wider dissemination. In round number terms about 100 charts are prepared for facsimile broadcast in a 24 hour period, including a substantial number of hand drawn products. These latter charts are prepared by forecasters at Bracknell, using forecast model products as a guide, along with other information such as satellite pictures and later observations. The final chart represents a 'man-machine mix', that is, a synthesis of computer speed and efficiency with human experience and intuition. Both hard-copy and VDU presentations are available to the forecaster at Bracknell (Figure 1) for the preparation of hand drawn products.

Three chart examples are shown in Figure 2, and other examples are to be found in companion papers. The computer drawn charts are produced on a Calcomp 1581 device, using a software package which extracts data from the comprehensive output data set (described earlier), and prepares it for either line drawing or grid plotting on a versatile range of chart areas

and projections. Tables 2 and 3 summarise the charts currently available on facsimile broadcasts. The more acceptable modern method of disseminating forecast data is by means of coded broadcasts, using higher speeds and enabling the transmission of a wider range of data. This system will be discussed in the next section.

4. Coded output

(a) Bracknell's dual role

The Meteorological Office at Bracknell has a dual function as far as the dissemination of coded forcast data is concerned. As a Regional Meteorological Centre (RMC) for Region VI of the World Meteorological Organisation (WMO), Bracknell makes available numerical analysis and forecast data covering Europe and the North Atlantic to other national meteorological centres. Acting as a World Area Forecast Centre (WAFC) of the World Area Forecast System (WAFS) initiated by the International Civil Aviation Organisation (ICAO), Bracknell provides data with a global coverage, both directly to airlines and also to regional centres of the WAFS. The provision of these data requires the use of agreed code forms, so that rapid transmissions from centre to centre are achieved without confusion or ambiguity of meaning.

(b) The code formats

The rapid progress in telecommunication techniques, leading to high speed lines and computer to computer connections, has resulted in a parallel development in the use of codes for transmitting numerical forecast data from one centre to another (Figure 1). The most widely used code form is WMO GRID-code (FM47- V) which was devised for use on low speed lines, using a character based format, with relatively high overheads associated with possible output on line printer devices. The majority of coded bulletins from Bracknell are in this format, and will remain so for the foreseeable future; however more efficient forms have been devised (see below) which should prove attractive enough for a major change in emphasis over the next five years. GRID-code forms the main-stay of the network between national weather centres in Region VI.

The data required for flight planning purposes by airlines has traditionally been supplied in Aviation Digital Forecast (ADF) code. ADF was designed for a specific purpose and thus differs from GRID-code (and its successors) in that the data are arranged in columns rather than in horizontal fields. The code uses a 'packed-decimal' format, ie more efficient than GRID-code, but is still character based and thus carries a large overhead penalty. Bracknell currently provides forecast data in this code form to British Airways, Scandinavian Airlines System, and the Societe Internationale de Telecommunications Aeronautiques.

In order to exchange the very large amounts of data required for the operation of the WAFS it was necessary that a much more efficient code form was devised. As an interim measure Bracknell and the National Meteorological Center in Washington developed a bit orientated code form, H-code, which was implemented between the two centres in 1984. Subsequently WMO has extended and developed the concept; a more widely agreed bit-orientated code GRIB (Gridded Binary) being ready for use at Bracknell since the 1st of January 1985. This bit-orientated code has been designed for use on fully automated computer to computer systems and is compatible with the more efficient telecommunication protocols required for transmission on high speed lines. The supply of data from Bracknell to automated systems (OASYS) at London Weather Centre and Heathrow Airport is an example of this computer to computer facility. The major part of the Bracknell coded products list can be made available in GRIB-code if required.

(c) Products available in code

Table 4 contains a concise summary of the products that are currently available in coded form from Bracknell. Three distinct classes of product are identified: those taken from the fine mesh NWP model, primarily for use in WMO Region VI; regional products from the global coarse mesh NWP model, again for use in Region VI and extending into the medium range; and global products from the coarse mesh model, formulated primarily for use in the WAFS but also available for

supply to other interested users. Details of the elements contained in the bulletins, areas covered, bulletin resolution and forecast times are all to be found in Table 4.

The most recent additions to this list of products are the very high resolution ($1\frac{1}{4}° \times 1\frac{1}{4}°$; every 3-hours) bulletins taken from fine mesh NWP model data. The Royal Netherlands Meteorological Institute (KNMI) requested such data for input to a scheme being for developed forecasting of maritime weather and sea state conditions along the Dutch coast. Other recent requests for data, which have been met by bulletins from the extensive range available at Bracknell, came from Zimbabwe, Mauritius and the Seychelles. Other requests, from Hong Kong for instance, are being examined but difficulties with telecommunication routes sometimes prevent rapid agreements being reached on the supply of coded data bulletins.

5. Back-up arrangements

Although modern computing systems are very reliable and have operational performance figures that approach 100% it is still inevitable that occasions will arise when the computing facilities at Bracknell, especially the Cyber 205 used for running the numerical models, are non-operational. At such times there is a need for reliable back-up arrangements, so that both chart and coded products can be supplied to the user without noticeable interruption. A computer outage of less than 12 hours is covered by ensuring that forecast data (in required formats) are routinely prepared for a period of 12 hours beyond that normally required.

By storing the data on the front end processing system it is then possible to supply operational users in a transparent manner, using results from a 12-hour old forecast run.

To ensure coverage beyond 12 hours there is a mutual exchange of global forecast data between Bracknell and Washington, using GRIB-code as a medium. Data from Washington arrive at Bracknell too late to be used operationally in real time, but after decoding and storage in a compatible output data set they can be used to give an almost complete range of products, although again from a 12-hour old forecast run.

The obvious omissions from the product list when operating in a back-up mode or those from the fine-mesh NWP model. Although in the recent past it has proved possible to run versions of the previous Bracknell NWP model on the front-end processors this is now considered to be increasingly unsatisfactory and other sources of high resolution forecast data are required. It is possible that other members of Region VI will be able to supply such data for back-up purposes.

Table 2(a)

Bracknell RMC

List of available chart products - using Analogue Facsimile transmissions

In the following tables all the computer produced charts are based on data from the Global NWP model. Most of the subjectively drawn charts (M) are also largely based on the products of the same model, or its derivatives.

(A) Analysis products

Field identifier	Reference time, and area of coverage 00	06	12	18	Method of production machine contours (C) manual input (M)
Surface pressure, with fronts and centres	F	F	F	F	M
	D				M
Height contours, 850, 700, 500, 300, 200 100, and 500-1000mb T'kness	A		A		C
Height contours 500mb	D				M
500mb contours and 500-1000mb T'kness	H		H		C
Sea surface temperature	M				M
Sea ice			E		M
State of sea	G		G		M

Table 2(b)

(B) Forecast products

Field identifier	Data time	Validity time (T+...hours) and area of coverage						Method of production machine contours (C), grid data (G)' manual input (M)
		18	24	48	72	96	120	
Surface pressure, with fronts and contours	00		F	C	C			M
	06		F					M
	12		F	C	C	C	C	M
	18		F					M
Height contours, 850, 700, 500, 300, 200, 1000mb	00		A					C
	12		A					C
500-1000mb T'kness	00		A					C
	12		A					C
Winds and temps (DDFFFTT) at 850, 700, 500, 400, 300, 250 & 200mb	00	K	K					G
	12	K	K					G
Winds and temps (DDFFFTT) at 500, 300, 250 & 200mb	00	B	B					G
	12	B	B					G
Significant weather (jets, tropopause, CAT etc)	00	B						M
	06	B						M
	12	B						M
	18	B						M
State of sea (wave height, direction)	00		G					M
	12		G					M

Table 3

BRACKNELL (RMC) List of chart areas

Area coverage

A:	Area:	48°N,145°W - 32°N,68°E - 18°N,12°E - 28°N,71°W - 48°N,145°W
	Projection:	Polar Stereographic
	Scale:	$1 : 20 \times 10^6$
B:	Area:	28°N,145°W - 24°N,54°E - 09°N,05°W - 02°N,84°W - 28°N,145°W
	Projection:	Polar Stereographic
	Scale:	$1 : 20 \times 10^6$
C:	Area:	42°N,90°W - 66°N,90°E - 30°N,20°E - 20°N,40°W - 42°N,90°W
	Projection:	Polar Stereographic
	Scale:	$1 : 30 \times 10^6$
D:	Area:	29°N,155°W - 28°N,63°E - 08°N,06°W - 08°N,85°W - 29°N,155°W
	Projection:	Polar Stereographic
	Scale:	$1 : 30 \times 10^6$
E:	Area:	57°N,96°W - 71°N,71°E - 46°N,14°E - 38°N,48°W - 57°N,96°W
	Projection:	Polar Stereographic
	Scale:	$1 : 10 \times 10^6$
F:	Area:	69°N,111°W - 37°N,50°E - 19°N,10°E - 34°N,55°W - 69°N,111°W
	Projection:	Polar Stereographic
	Scale:	$1 : 20 \times 10^6$
G:	Area:	42°N,112°W - 60°N,32°E - 28°N,10°W - 21°N,74°W - 42°N,112°W
	Projection:	Polar Stereographic
	Scale:	$1 : 20 \times 10^6$
H:	Area:	80°N,05°W - 44°N,32°E - 28°N,05°W - 43°N,41°W - 80°N,05°W
	Projection:	Polar Stereographic
	Scale	$1 : 20 \times 10^6$
K:	Area:	53°N,50°W - 53°N,65°E - 26°N,34°E - 26°N,18°W - 53°N,50°W
	Projection:	Polar Stereographic
	Scale:	$1 : 17 \times 10^6$
L:	Area:	31°N,20°W - 23°N,150°E - 6°S,102°E - 5°S,33°E - 31°N,20°W
	Projection:	Polar Stereographic
	Scale:	$1 : 36 \times 10^6$
M:	Area:	67°N,37°W - 70°N,18°E - 47°N,07°E - 45°N,19°W - 67°N,37°W
	Projection:	Polar Stereographic
	Scale:	$1 : 5 \times 10^6$

Table 4

LIST OF AVAILABLE FORECAST FIELDS FROM BRACKNELL

Forecast runs are made from both 00Z and 12Z data time. Bulletins are coded in WMO GRID (FM47-V)). Details of bulletin headings and contents can be supplied on request, including details of GRIB-code bulletins.

	Regional Fine-Mesh Products	Regional Coarse-Mesh Products	Global Coarse-Mesh Products
Elements:	Surface pressure, surface wind (10 m), accumulated precipitation. Heights, winds and temperatures for 850 and 500 hPa.	Surface pressure, surface wind (10 m) Heights, winds and temperatures at 850, 700, 500, 400, 300, 250, 200, 150, 100 hPa.	Surface pressure, surface wind (10 m) 500 hPa height Maximum wind and tropopause Winds and temperatures at 850, 700, 500, 400, 300, 250, 200, 150, 100 hPa.
Areas:	The 3 areas all span $32^1/_2$°N to 75°N. The longitudes covered are 70°W to 35°W (area W or 255), 35°W to 0° (area X or 256), 0° to 35°E (area Y or 257).	There are 5 areas. Four span 25°N to 75°N, the longitudes are 90°W to 45°W (area Z or 205), 45°W to 0° (area N or 206), 0° to 45°E (area O or 207), 45°E to 90°E (area P or 208). The fifth area (area I or 201) covers 75°N to 90°N and 90°W to 90°E.	There are 16 areas. In each hemisphere there are two polar areas covering latitudes 70° to 80° and 80° to 90° and 4 mid-latitude areas spanning 20° to 70° in quadrants. A further 4 areas spanning 20°N to 20°S cover the tropical belt.
Resolution:	The data are normally supplied on a latitude-longitude grid at $2^1/_2$° resolution. $1^1/_4$° resolution is available if required for fields of surface pressure, wind and precipitation	The data are supplied on a latitude-longitude grid with a $2^1/_2$° resolution. For the polar area (area 201), the resolution is $2^1/_2$° latitude by 10° longitude.	The mid-latiude areas are at a resolution of $2^1/_2$° latitude by 5° longitude; the tropical belt is at 5° latitude by 5° longitude. In the polar regions there is reduced longitudinal resolution.
Forecast Times:	Fields are available at 6-hour intervals from the analysis (T+0) to a forecast time of T+36. Fields of surface pressure, wind and precipitation are available at 3-hour intervals on the finer grid.	Fields are avialable at the following forecast times T+0, T+6, T+12, T+18, T+24, T+30, T+36, T+42, T+48, T+60, and T+72. In addition surface pressure and 500 hPa height are available at T+96 and T+120.	Fields are available at 6-hour intervals from the analysis (T+0) to a forecast time of T+48. In addition surface pressure and 500 hPa height are available at T+60, T+72, T+96 and T+120.

FIGURE 1

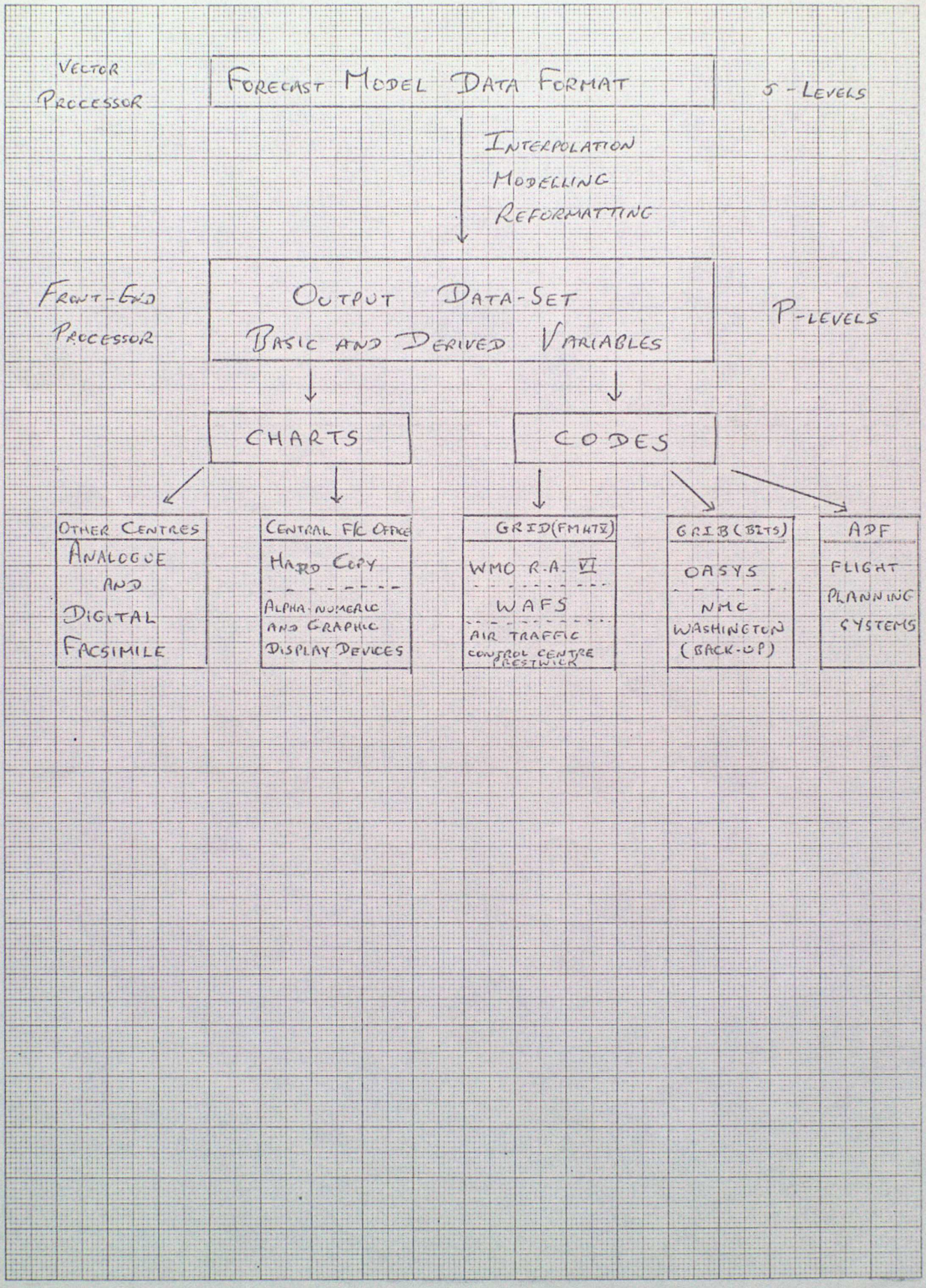

Fig 2

Fig 2.

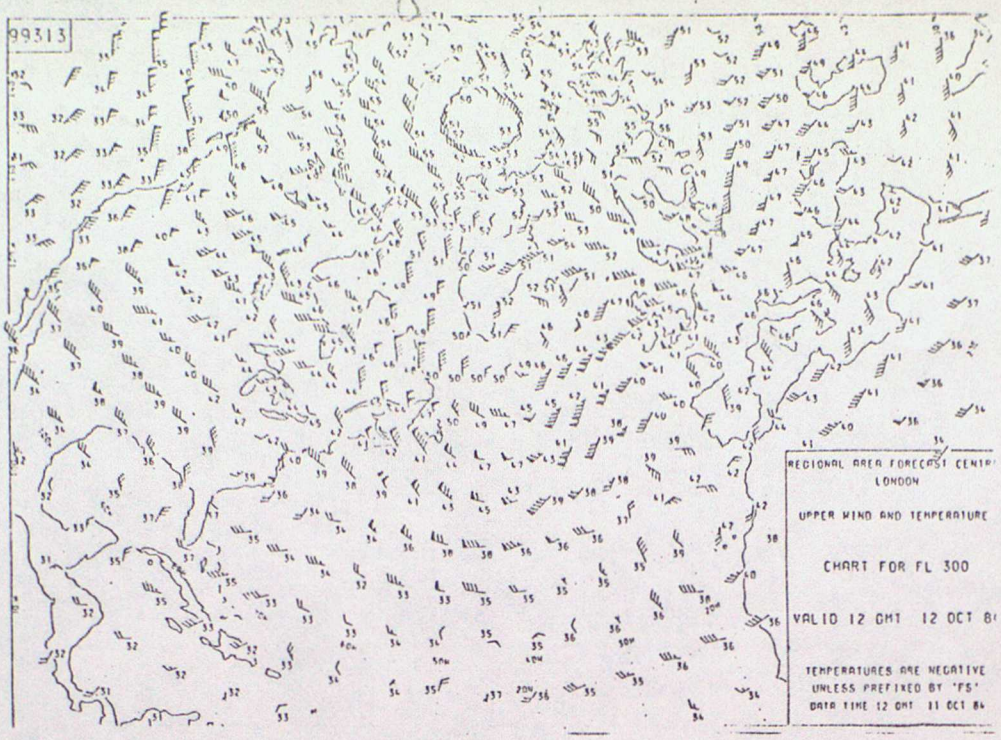
99313
REGIONAL AREA FORECAST CENTRE
LONDON
UPPER WIND AND TEMPERATURE
CHART FOR FL 300
VALID 12 GMT 12 OCT 8
TEMPERATURES ARE NEGATIVE
UNLESS PREFIXED BY 'PS'
DATA TIME 12 GMT 11 OCT 84

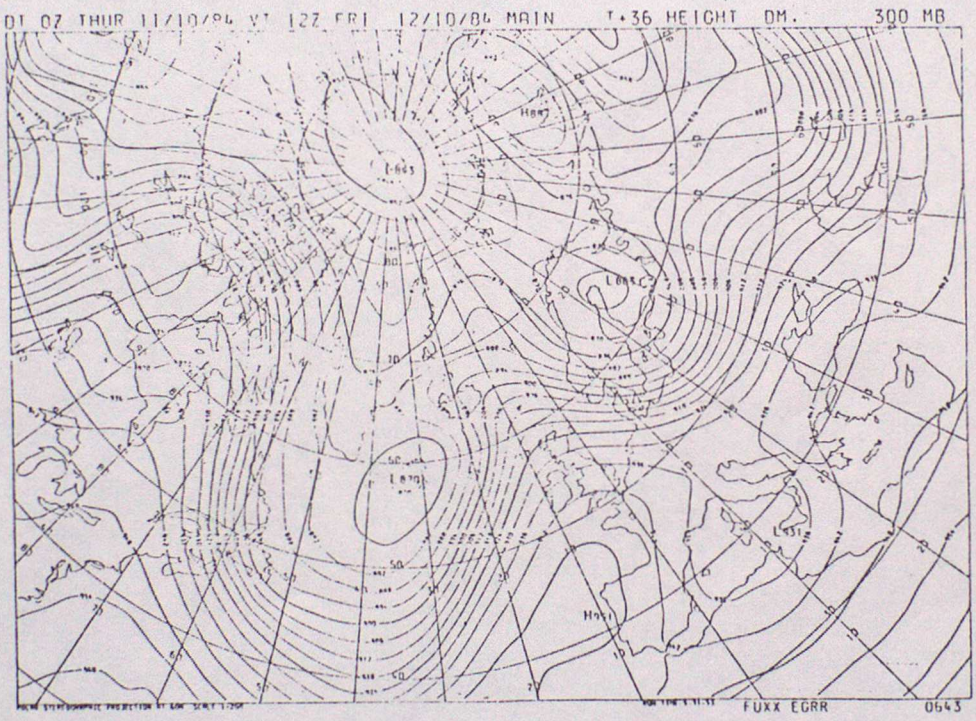
DT 0Z THUR 11/10/84 VT 12Z FRI 12/10/84 MAIN T+36 HEIGHT DM. 300 MB
FUXX EGRR 0643

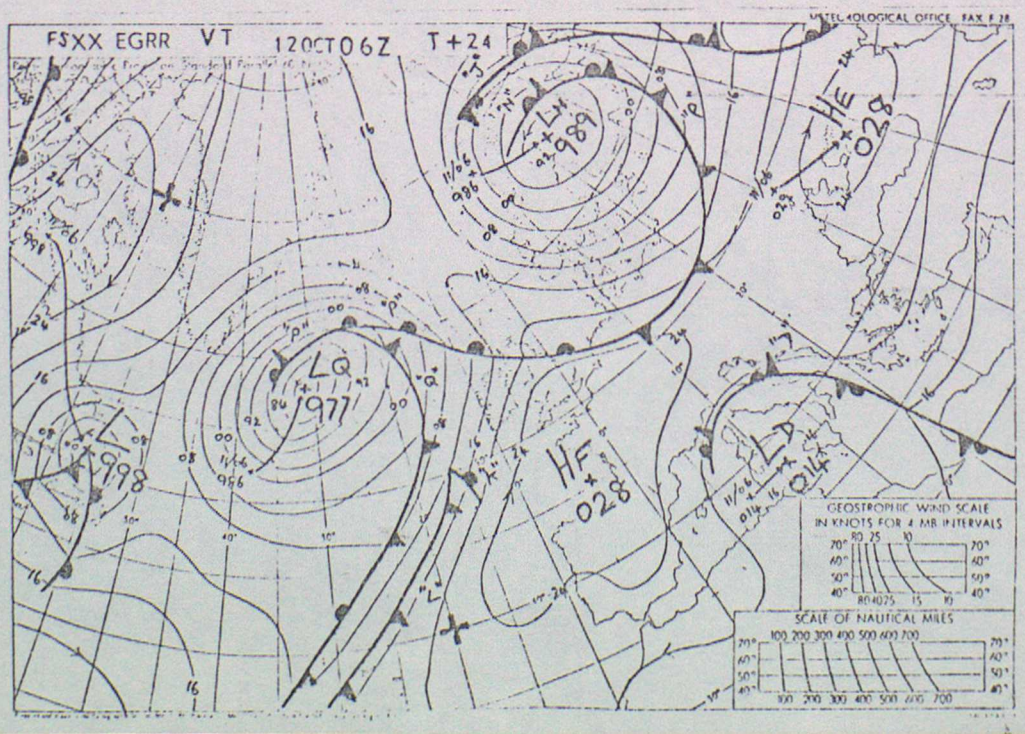
METEOROLOGICAL OFFICE FAX F 28
FSXX EGRR VT 120CT06Z T+24
LM 989
HE 028
LQ 977
HF 028
LD 014
L 998
GEOSTROPHIC WIND SCALE
IN KNOTS FOR 4 MB INTERVALS
SCALE OF NAUTICAL MILES

ADVANCED LECTURES 1985

OPERATIONAL NUMERICAL WEATHER PREDICTION

Lecture 8

Wave and swell prediction

J J Ephraums

1. Ocean waves

a. Observed features of wave evolution

i. **Light winds:** When the wind starts blowing over a calm sea, small ripples occur. These are capillary waves, whose restoring force is surface tension. As the wind increases in strength, larger and longer waves begin to form - gravity waves. In a moderate breeze the wave field is observed to be essentially random with a mean direction of propagation along the wind direction and a mean height which increases rapidly with higher wind speeds.

ii. **Fresh winds:** In a fresh breeze, individual waves are seen to break at the crests and form foaming 'white horses', a mechanism which limits the wave steepness. Nevertheless a growing 'wind-sea' is characterised by choppy, short, steep waves. Ocasionally waves will group together and form a much larger 'freak' wave than the average. The wave height depends on the duration and fetch of the wind. Fig 1a.

iii. **Storms:** In strong gales the waves become huge and the sea surface is whipped by spray from breaking crests. The so called 'freak wave' in these cases is dangerous because of its characteristically steep forward face which slams structures and buries ships. For a given wind speed the waves seem to become 'fully developed after sufficient length of time and stop growing.

iv. **Swell:** When storm winds subside the shorter wavelength waves decay rapidly leving longer smoother swells to propagate out with little or no attenuation before reaching shores over 1000 miles away. Due to dispersion the period of arriving swell decreases with time since longer waves travel faster. Fig 1b.

v. **Shallow water:** As waves and swell reach shallow tidal waters several modifying processes begin to act. As the water depth becomes comparable to the wavelength, waves 'feel' the sea bottom and lose height through bottom friction. Waves travelling at an angle to depth contours are refracted and may produce caustics of high waves at headlands. The group velocity of waves decreases in shallower water, causing the waves to slow down and bunch up, or 'shoal'. Waves become steeper and choppy, often breaking - a sure sign of submerged reefs or sandbars, and a hazard to small craft. Fig 1c. As waves travel up a beach they break, though whether they spill gradually at crests or crash onto the beach at the last minute depends on whether the beach is gently or steeply shelving. Breaking surf produces a 'set-up' of the water level at the beach increasing the likelihood of damage or flooding. Figs 1d, 1e.

vi. **Tides and Currents:** The diurnal cycle of tides causes changes in sea depth which in turn produces a varying pattern of coastal waves as refraction, shoaling and surf breaking become more or less pronounced through the day. Tidal currents can

oppose waves and produce shoaling, as can the outflow of an estuary. Fig 1f, 1g. Surf produces both long shore currents responsible for coastal erosion, and offshore 'rip' currents which can rapidly carry the unwary swimmer out to sea. The narrow rip can only be escaped by swimming parallel to the shore before attempting to swim back to the beach. In theory waves can be refracted by currents, or even suffer total internal reflection but this has not been observed.

b. Measurements and Empirical Facts

i. **Measuring systems:** Most real time measurements of waves are visual estimates reported from oil platforms, weather ships and ships of passage. These are not accurate enough to provide quantitative information on wave processes. The most popular measuring device is an accelerometer contained in a 'waverider' buoy, which yields a time history of sea surface elevation after integrations of the device signal.

The significant wave height (H_S or $H_{1/3}$) is then defined as the mean of the highest one third of all the waves - usually taken over a fifteen minute interval. Note that wave heights are measured trough to crest!

Other techniques for measuring waves are satellite based altimeters and synthetic aperture radars, and land based long wave radar which relies on Bragg reflection from waves with wavelengths comparable to the radar. All these methods are still considered to be research concepts and are a long way from being viable operational systems.

ii. **Spectral Analysis:** A single property of the wave field, such as H_S, is insufficient to fully describe the distribution of wave heights and periods. It is therefore necessary to perform a Fourier analysis of the height record and to produce a wave spectrum, which for the purpose of wave modelling is chosen to be of wave energy ($\propto$ amplitude^2) against frequency (see Fig 2). Subsequent integration of the energy spectrum then yields the wave height H_S

$$E = \iint E(f,\theta)\,df\,d\theta, \qquad H_S = 4\sqrt{E}$$

Other quantities can be derived from appropriate moments of the spectrum.

iii. **Spectral Evolution:** The JONSWAP project (Hasselmann, 1973) produced the first detailed measurements of the wave spectrum in a growing wind sea. (Fig 3). Note how the total energy increases with fetch, and that the peak frequency migrates to lower values. We have already observed this in (a). In particular it was found that the spectral shape of a growing wind sea could be represented by a universal spectral shape (Fig 4) namely

$$F(f) = \frac{\alpha g^2}{(2\pi)^4 f^5} \exp\left[-\frac{5}{4}\left(\frac{f}{f_m}\right)^{-4} + \ln \Omega . \exp\left(-\frac{(f-f_m)^2}{2\sigma^2 f_m^2} \right) \right]$$

This consists of three terms:

- an f^{-5} term which produces a high frequency tail independent of total energy.
- an exponential term which produces a low frequency cut off.
- a super exponential which makes the spectrum more 'peaky' in the early growth stages.

The peak frequency f_m, α, and Ω all depend on the wind speed (u) at 19.5 m and the total wave energy E. In 1960 a wave spectrum for a 'fully developed sea' had been proposed by Pierson and Moskowitz - this corresponds to the above with $\Omega = 1$, when $E = E_{PM}$.

$$E_{PM} = 2.8 \times 10^{-5}\, U^4 \quad \rightarrow \quad H_{PM} = 0.021\, U^2 \text{ or } \frac{U^2}{50}$$

So for a fully developed sea from 20 m/s wind the significant wave height is 8 metres.

Notice that this is only a description of the frequency distribution of wave energy F(f). It is very difficult to measure the full 2-dimensional spectrum $E(f,\theta)$ so it is assumed that

$$E(f,\theta) = F(f)G(\theta)$$

$G(\theta)$ is not known exactly and is frequently assumed to take the form

$$G(\theta) = \cos^2(\theta - \psi)$$

where ψ is the wind direction.

These spectral functions are attempts by workers to categorise hundreds of measured spectra in order to simplify wave prediction and to facilitate the formulation of physical processes responsible for them.

Likewise, measurements of wave energy with fetch appear to yield a universal growth law after non-dimensional scaling. Despite the scatter in these results such 'laws' are used frequently for wave model tuning. Fig 5 shows a comparison of 10 operational wave models in trying to reproduce measured growth rates under idealised situations. This illustrates the lack of knowledge and understanding of even quite 'simple' wave mechanisms at the current time.

c. Useful equations describing waves

i. Sinusoidal waves

Wavelength = L
Wavenumber = $k = 2\pi/L$
Phase velocity = C
Group velocity = C_g

	SHALLOW WATER	DEEP WATER
Depth (H)	$L/25<H<L/2$	$H>L/2$
Wavenumber	$2\pi f=(gk \tanh kH)^{1/2}$	$2\pi f=(gk)^{1/2}$
Phase velocity	$c = (g \tanh (kH)/k)^{1/2}$	$c = g/2\pi f$
Group velocity	$c_g = 1/2(\frac{g}{k} \tanh(kH))^{1/2}(1+\frac{2kH}{\sinh KH})$	$c_g = g/4\pi f$

ii. The Energy Balance Equation

In shallow water the evolution of the wave energy spectrum is assumed to obey.

$$\frac{\partial E}{\partial t} + \nabla.(\underline{c}_g E) + \frac{\partial}{\partial \theta}(\underline{c}_g.\nabla\theta)E = S_{tot} \qquad E=E(f,\theta)$$

The second (advective) and third (refractive) terms can lead to 'shoaling', since a decrease in c_g over a pathlength for example will led to an increase in E if the flux is to remain constant.

S_{tot} represents all processes by which energy is gained or lost by a spectral component $E(f,\theta)$. It is further assumed that (Fig 6).

$S_{tot} = S_{wind} + S_{dis} + S_{nl} + S_{bot}$ for that component.

where S_{wind} = energy input due to the wind
S_{dis} = energy lost from waves due to whitecapping.
S_{nl} = energy redistributed within the spectrum via conservative nonlinear interactions. Shapes the spectrum.
S_{bot} = energy extracted from waves through bottom friction in shallow ater.

Fig 7 shows these source functions derived from measured wave spectra in shallow waters during a North Sea storm. The waves were in equilibrium such that $S_{tot} \approx 0$ and no growth or decay was observed. Note that S_{nl} feeds energy from high to low frequencies, producing a spectral evolution already shown in

Fig 2. S_{nl} is a highly complex function which cannot be computed efficiently and thus has to be parameterised by ensuring that the spectral shape conforms to that defined in Fig. 3.

Typically $S_{wind} = \beta f E(f,\theta) \left(\frac{U}{C} \cos(\theta-\psi)-1\right)$

β can be tuned for optimum wave growth U and ψ are wind speed and direction, so the term in brackets restricts wave growth to components travelling slower than the wind speed resolved along their direction of propagation. The term is set to zero if the waves travel faster than the wind. The higher frequencies grow faster, but $E(f,\theta)$ is restricted by the transfer of energy to lower frequencies.

This term has been established from measurements and theory. S_{dis} on the other hand is less well known and is usually chosen by the modeller. An accepted form is

$$S_{dis} = -\delta T(E) f^2 E(f,\theta)$$

where $T(E)$ is a function of the entire spectrum and δ is a tuning constant. Higher frequencies will suffer greater dissipation, and more so if waves are higher overall.

$$S_{bot} = -\phi g k^2 \langle u \rangle E(f,\theta)/(2\pi f \cosh kH)^2$$

ϕ is dependent on the composition and structure of the seabed, and is chosen by the modeller. $\langle u \rangle$ is the integrated bottom motion of the waves. S_{bot} preferentially damps long wavelength waves as we would expect.

In deep water we rarely get an implicit energy balance between input and dissipation with these source functions at very long fetches/duration so a limit is stipulated to prevent waves growing beyond a Pierson-Moskowitz (fully developed) spectrum.

2. Operational wave models

i. **Model construction:** The wave field is represented by a regular polar-stereographic grid of points at which the wave energy spectrum is held as a discrete array of 14 frequency and 16 direction components. A high spectral resolution is required to model accurately the frequency and directional evolution of the spectrum. Advection is performed independently on each component using a modified 4th order Lax-Wendroff finite difference scheme. The

external source functions are modelled using forward time differencing. The internal, non-linear, source function is modelled by simply redistributing energy within the wind sea spectrum to achieve the required spectral shape whilst conserving energy. The high resolution continental shelf model contains a detailed model coastline and accurate bottom topography but cannot model very local shallow water processes or beach conditions.

ii. **Wind input:** Winds are extracted directly from the coarse or fine mesh 15 level NWP model at the sigma level 0.997. This corresponds closely with the nominal wind input level of 19.5 m in the models; the winds are not adjusted in any way before input.

iii. **Boundary values:** The fine mesh model takes its boundary data from the appropriate coarse mesh points, enabling distant Atlantic swell to propagate into the Continental Shelf area.

iv. **Wave analysis:** There are insufficient wave data to perform a wave analysis with which to start a forecast. Instead a wave 'hindcast' is performed which reruns the previous 12 hour forecast with corrected forecast wind fields. These wave hindcasts are archived every 12 hours providing a valuable data base of wave information for development work, verification, commercial enquiries and climatology.

v. **Verification:** Daily verification is performed operationally from weather ships and oil platform data. Fig 10 shows an example of wave and wind errors at a North Sea oil platform. Wave errors are dependent on wind errors at a given location, but additional errors are introduced through incorrect swell prediction, presumably attributable to wind errors further afield.

3. Future developments

i. **Hindcasting:** Wave models are becoming more important in their non-operational roles. One of these is in the creation of a synthetic wave climate using reconstructed historical wind fields, either for individual storms or long periods. Fig 8 shows a hindcast wave spectrum using the Met Office model.

ii. **Data Assimilation:** The advent of satellite wave mesurements from ERS-1 will open up the possibility of assimilating high quality wave data in model analyses. Work has just started in this subject, motivated by the formation of a European Wave Modelling Group (WAM) which is also trying to develop a rigorous scientific wave prediction model based on the explicit representation of all the source terms.

iii. **Global model:** Work has begun on a global wave model to take advantage of the global coverage of NWP forecast winds. The model will be on a lat-long grid and will also include a great circle correction term for swell propagation. Applications include ship routeing and an incresing demand for forecasts for the offshore industry in such locations as the South China Sea.

iii. **Surge Modelling:** At present the Met Office runs an operational storm surge prediction model developed by IOS. A possible future development is a combined interactive wave-surge prediction model.

4. Further reading

Barnett, T.P., Kenyon, K.E. Recent advances in the study of wind waves. Rep. Prog. Phys. 38, (1975).

Beer, T. Environmental Oceanography. Pergamon Press (1983).

Draper, L and Bownass, T.M. Wave devastation behind Chesil Beach. Weather 38 (1983).

Francis, P.E. An introduction to the Met Office wave forecast model. Met O 2b TN 72 (1984).

Golding, B. A wave prediction system for real-time sea state forecasting. Quart. J.R. Met. Soc. 109 (1983).

Hasselmann, K. et al. Measurements of wind-wave growth and swell decay during the JONSWAP project. Deut. Hydrogr. ZA12 (1973).

Houghton, I. A long timeseries verification of hindcasts from the Meteorological Office wave model archive. Met. Mag. 113 (1984).

Kinsman, B. Wind waves. Prentice-Hall (1965).

Phillips, O.M. The dynamics of the upper ocean. Cambridge UP. (1966).

SWAMP Group. An intercomparison of wind-wave prediction models, Part 1. Proc IUCRM Symp on wave dynamics and radio probing of the ocean surface, Miami. Plenum Press (1984).

SWIM Group. A shallow water intercomparison of three numerical wave prediction models. To be published in Quart. J.R. Met. Soc.

Tucker, M.J. Observation of ocean waves. Phil. Trans. R. Soc. Lond. A309 (1983).

Figure 1

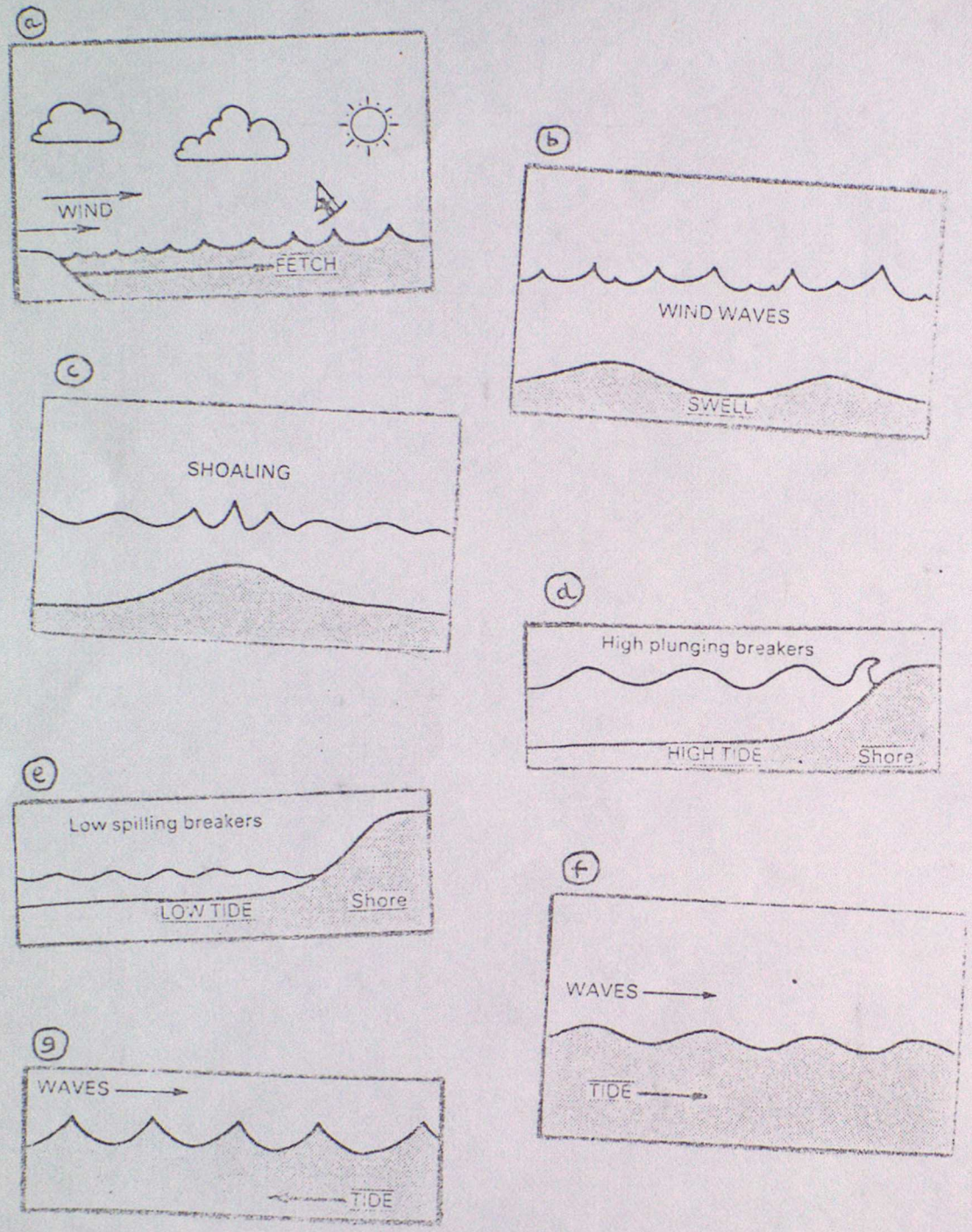

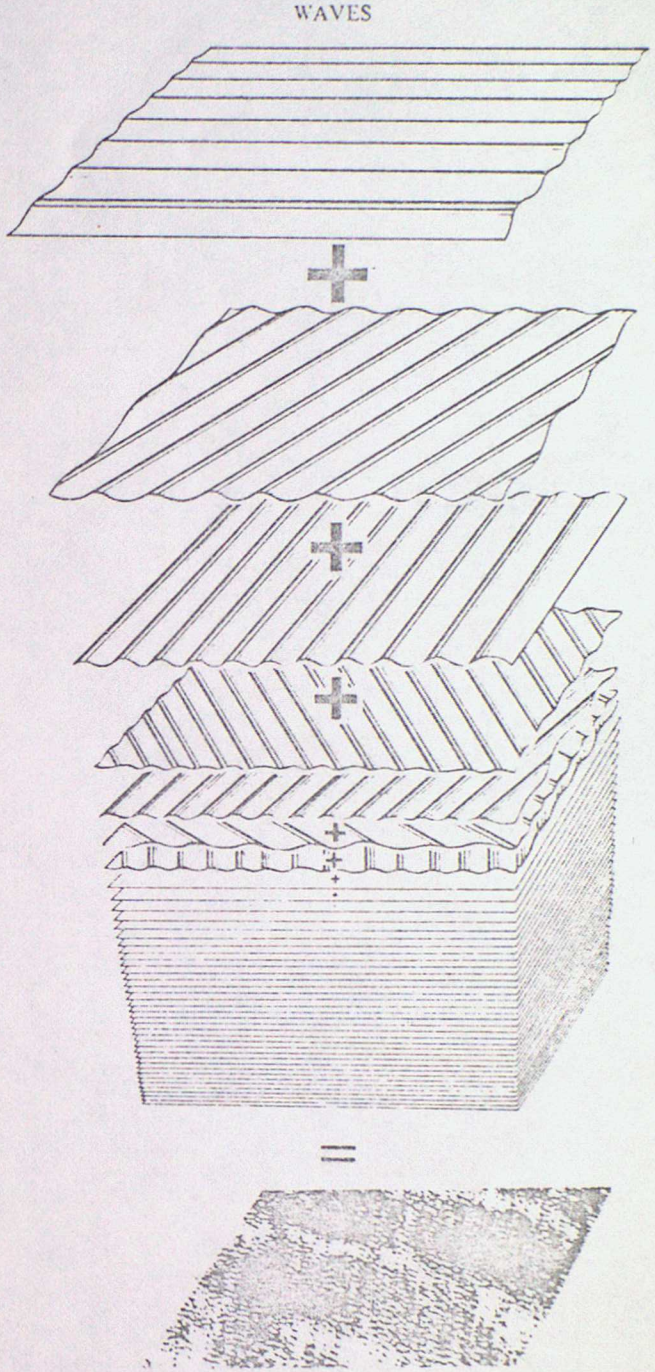

FIG. 2 *The sea surface can be represented by the sum of many simple sinusoidal wave trains of different periods and amplitudes moving in different directions.*

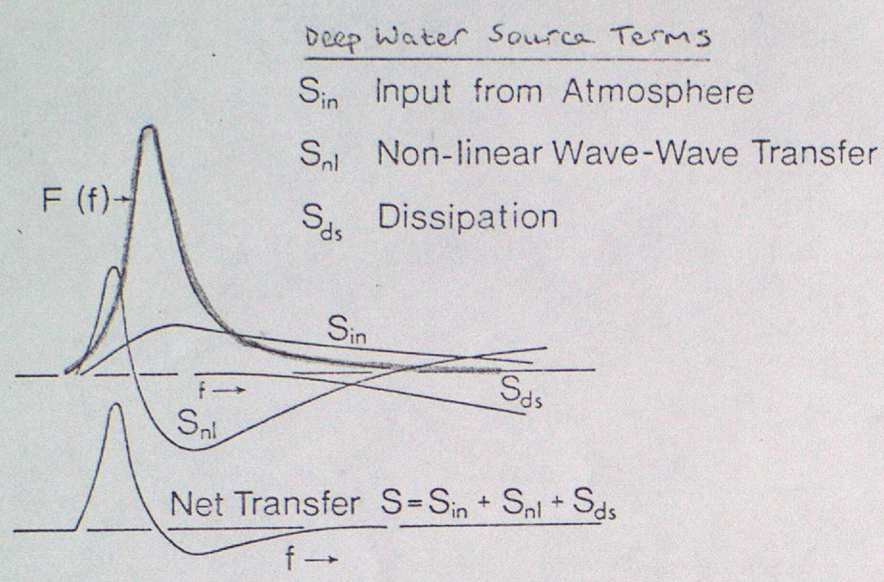

Fig. 6 Schematic energy balance for a developing wind-sea after Hasselmann et al. (1973). F(f) is the one dimensional wave spectrum.

Figure 7

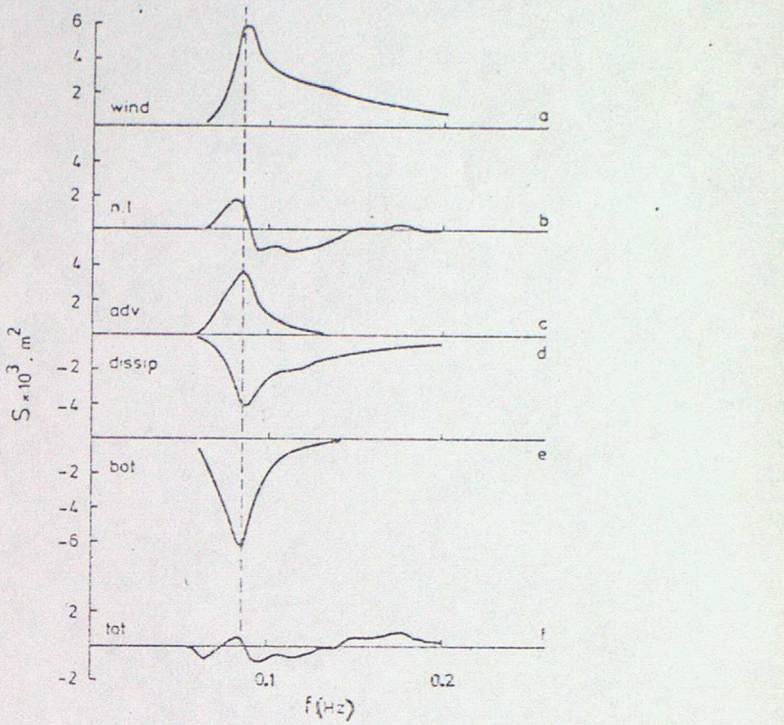

Figure 8

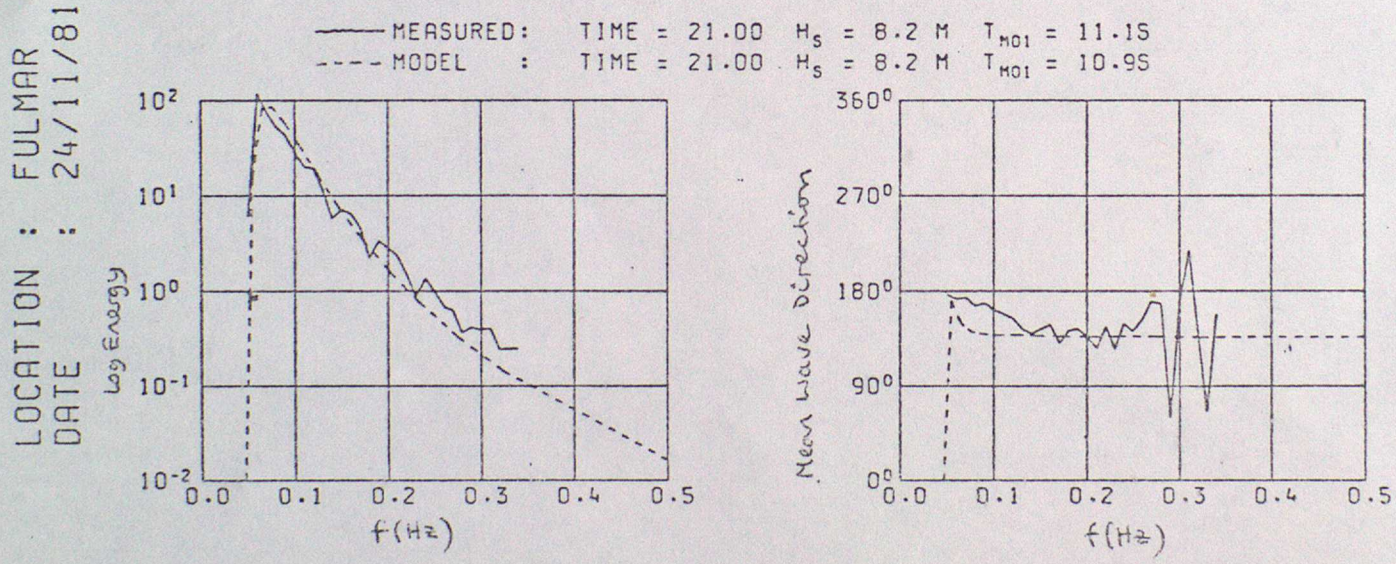

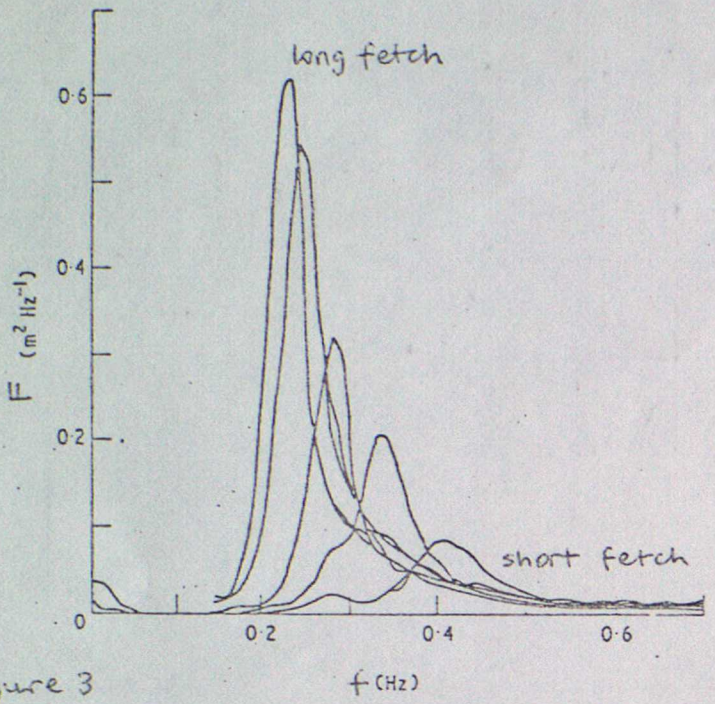

Figure 3

Evolution of the wave spectrum with fetch for offshore wind.

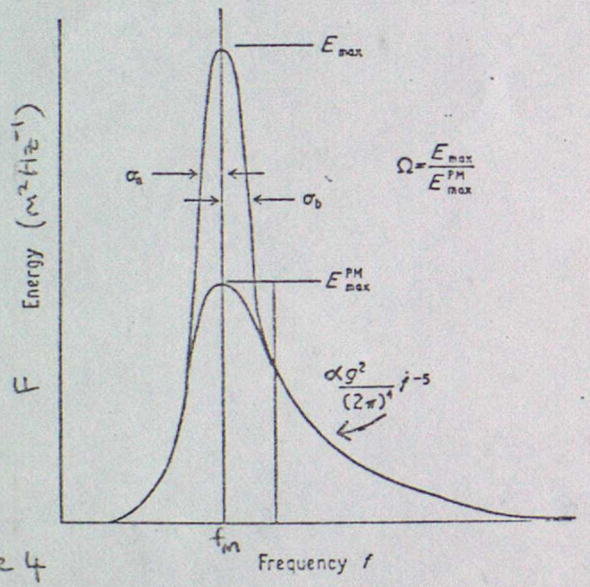

Figure 4

Schematic view of the best-fit fetch-limited spectrum obtained during the JONSWAP project. Definition of the free parameters and the functional fit is illustrated in the figure.

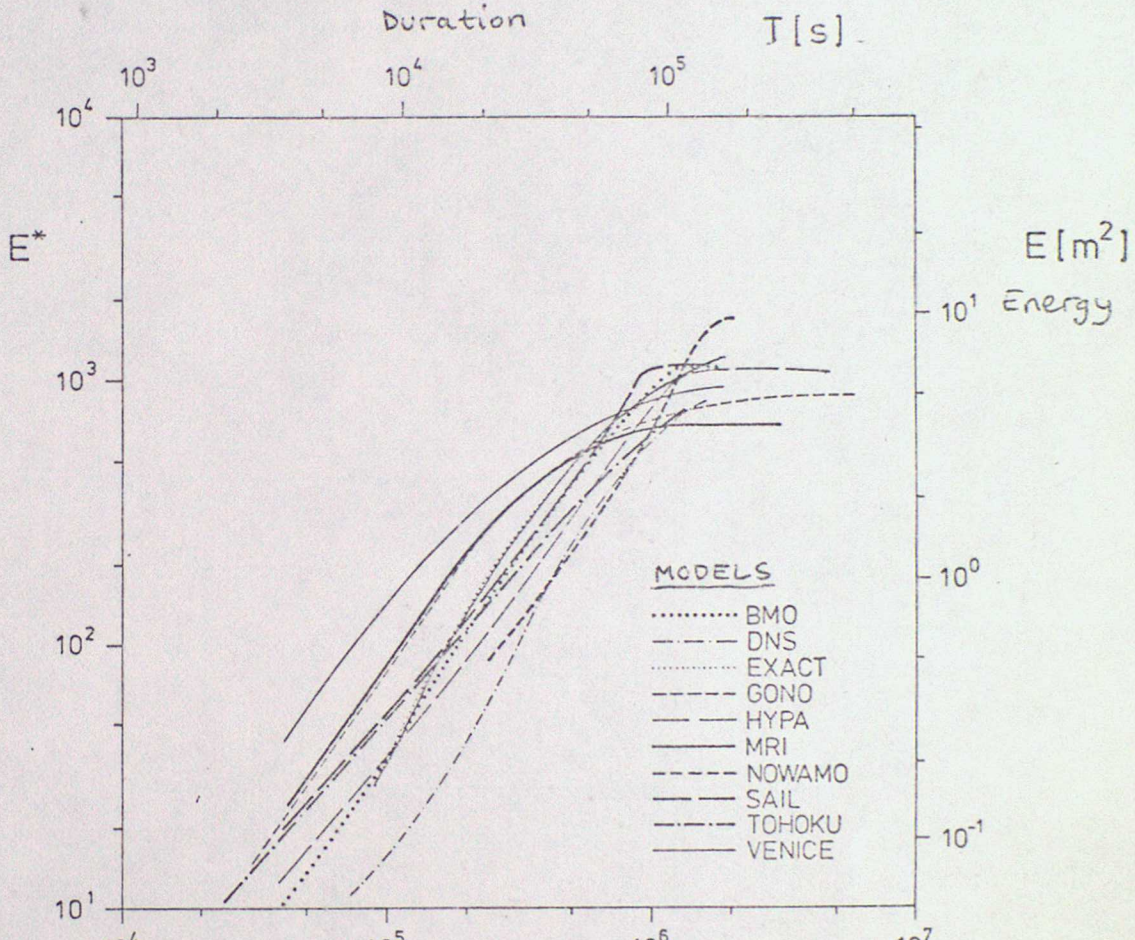

Figure 5

Figure 9 OPERATIONAL WAVE MODEL

MODEL	OUTLOOK	GRIDLENGTH	WINDS	APPLICATIONS
Northern Hemisphere	3 days	150 km	Coarse mesh every 1½hours	Ships routeing (manual/numerical) Boundary values (Continental Shelf) RMC radio facsimile charts Archive
Continental Shelf	36 hours	25 km	Fine mesh every ½ hour	Offshore operations Towing advice Coastal flood warning Design & environmental studies Ship routeing Archive
Mediterranean	36 hours	50 km	Fine mesh every ½ hour	Offshore operations Towing advice Ships routeing Archive

Figure 10

BRENT B.FINE MESH

CORRELATION COEFFICIENT: 0.3

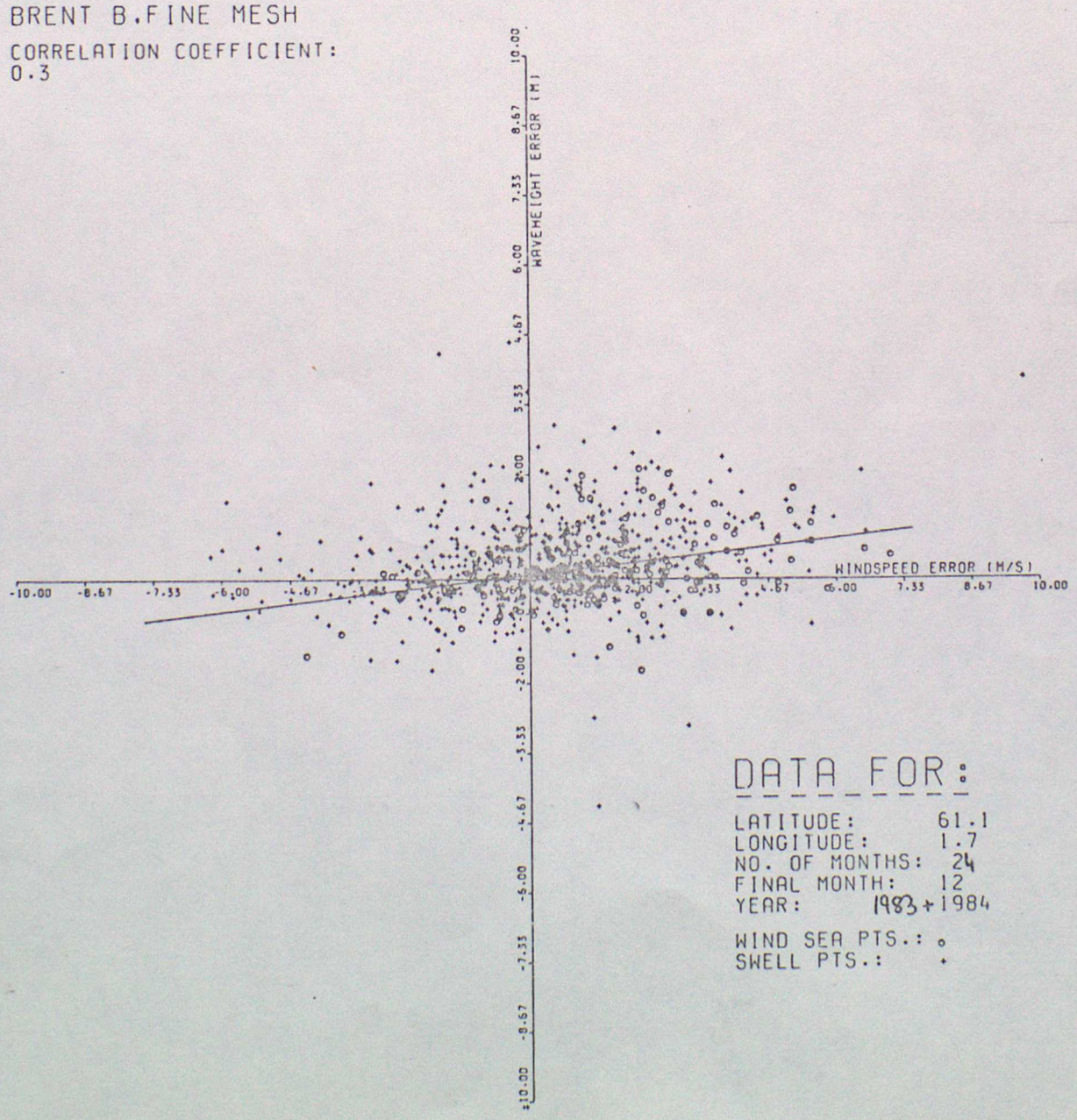

WAVE AND SURGE MODEL OUTPUT APPLICATIONS

FLOOD WARNING

FOR TRANSMISSION TO SOUTHERN WATER AUTHORITY VIA MET.O.5

INITIAL DATA TIME 12Z 8/ 4/83

LOCATION 50.6N 0.8E

HOURS AFTER DATA TIME	WIND SPEED KTS	WIND DIRECTION DEG(FROM)	TOTAL WAVES HEIGHT M	TOTAL WAVES PERIOD SECS	WIND SEA HEIGHT M	WIND SEA PERIOD SECS	SWELL HEIGHT M	SWELL PERIOD SECS	SWELL DIRECTION DEG(FROM)
0.0	13.6	255.	1.3	4.9	0.9	3.8	1.0	7.3	250.
3.0	17.0	240.	1.5	4.9	1.2	4.2	0.9	7.6	247.
6.0	12.8	233.	1.5	4.9	1.2	4.4	0.8	7.6	241.
9.0	7.0	233.	1.4	5.1	0.4	3.1	1.3	5.4	242.
12.0	6.8	250.	1.3	5.5	0.0	0.0	1.3	5.5	244.
15.0	5.9	250.	1.3	6.0	0.0	0.0	1.3	6.0	247.
18.0	6.5	245.	1.3	6.3	0.0	0.0	1.3	6.3	248.
21.0	9.3	246.	1.3	6.3	0.1	3.1	1.3	6.4	249.
24.0	13.4	246.	1.3	5.7	0.5	3.5	1.3	7.0	249.
27.0		248.	1.3	5.5	0.6	3.4	1.2	7.1	248.
30.0		251.	1.2	6.2	0.0	0.0	1.1	6.2	245.
33.0			1.1	6.1	0.0	0.0	1.2	6.1	244.
36.0				6.2	0.0	0.0	1.1	6.2	245.

STORM SURGE FORECAST. RESIDUAL ELEVATIONS IN METRES. DATA STARTS AT 0 HRS GMT 29/ 8/1984

GMT	585 STWY	548 WICK	726 ABDN	991 NSHL	1214 IMMI	1258 WASH	1349 LOFT	1436 FXST	1479 SHNS	1484 VLIS	1441 HOEK	1267 DHEL	1227 BORK	1186 CUXN	966 ESBG
0															
100	.09	.13	.12	.06	.01	.00	-.06	-.12	-.15	-.13	-.10	-.05	-.05	-.05	-.01
200	.06	.15	.11	.05	-.00L	-.01	-.05	-.10H	-.13	-.11	-.10	-.06	-.07	-.07H	.02
300	.06	.14	.11H	.06	-.02	-.03L	-.05	-.06	-.10H	-.08	-.09	-.01	-.04	-.05	.03
400	.09L	.11	.09	.08	-.01	-.06	-.06	-.07	-.06	-.08H	-.08	-.00L	.01	.01	.01
500	.13	.09	.10	.06H	.01	-.05	-.04	-.07	-.05	-.07	-.06H	-.01	.02	.01	.04H
600	.18	.14	.08	.06	.03	-.04	-.04	-.07	-.07	-.04	-.05	.00	.02L	.02	.09
700	.13	.13L	.11	.08	.03	-.01	-.03	-.08	-.09	-.02	-.02	.02	.03	.06	.10
800	.07H	.15	.09	.08	.04H	.02	-.03	-.09L	-.10	-.01	.02	.06	.05	.07	.12
900	.10	.14	.10	.05	.06	.04H	-.01	-.07	-.12L	-.01	.02	.10H	.09	.08L	.15
1000	.18	.13	.08L	.05	.06	.06	.00	-.06	-.15	.00L	.04L	.11	.13	.15	.18L
1100	.24	.10	.08	.04	.09	.06	-.00H	-.04	-.14	.03	.07	.12	.14	.18	.20
1200	.22	.11	.06	.04L	.09	.06	.02	-.04	-.11	.04	.07H	.13	.13H	.15	.21
1300	.16	.15	.09	.04	.07	.07	.05	-.01	-.06	.03	.07L	.14	.15	.16	.22
1400	.12	.18H	.11	.03	.06	.05	.09	.04H	-.01	.02		.13	.18	.19H	.26
1500	.15L	.19	.13	.04	.07	.04	.07	.06	.02			.14	.19	.19	.32
1600	.20	.20	.12H	.04L	.06	.03L	.06	.07				.15	.24	.24	.32
1700	.26	.18	.13	.07	.04	.02	.06					.17	.28	.28	.25H
1800	.27	.18	.13	.07	.03							.17L	.26	.20	.20
		.22	.12	.07H	.01								.22	.21	.21
				.04	.02										

FLOOD WARNING

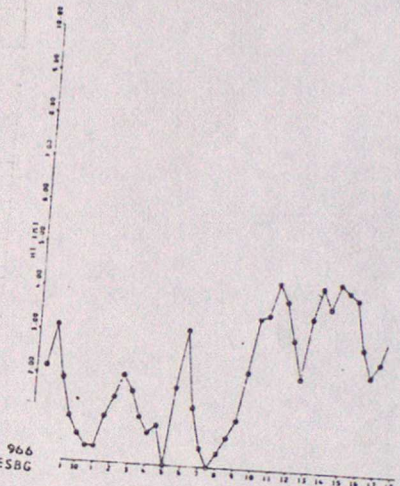

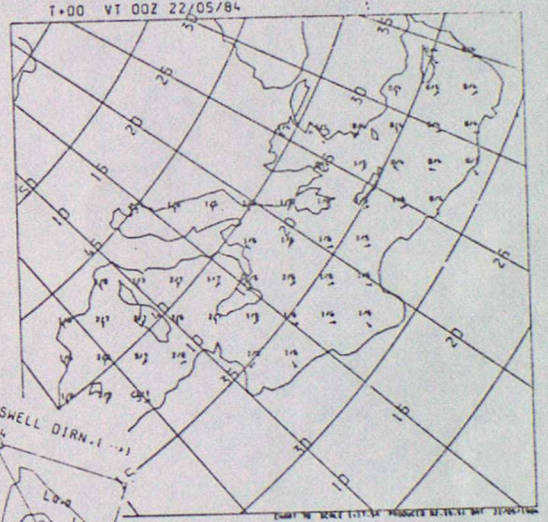

ARCHIVE

TOWING ADVICE

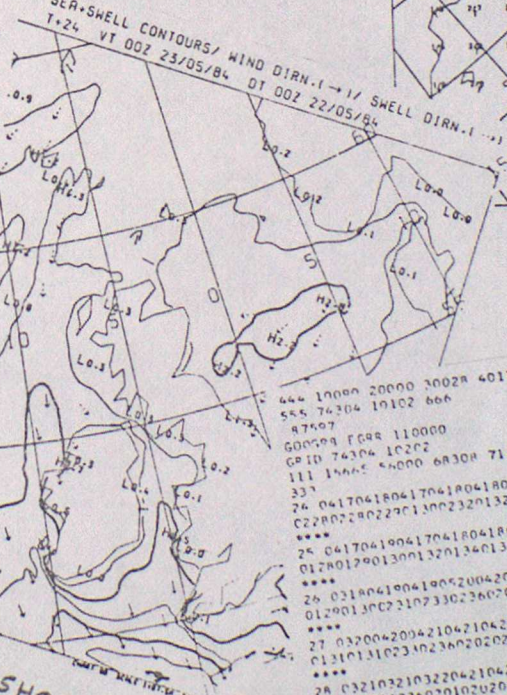

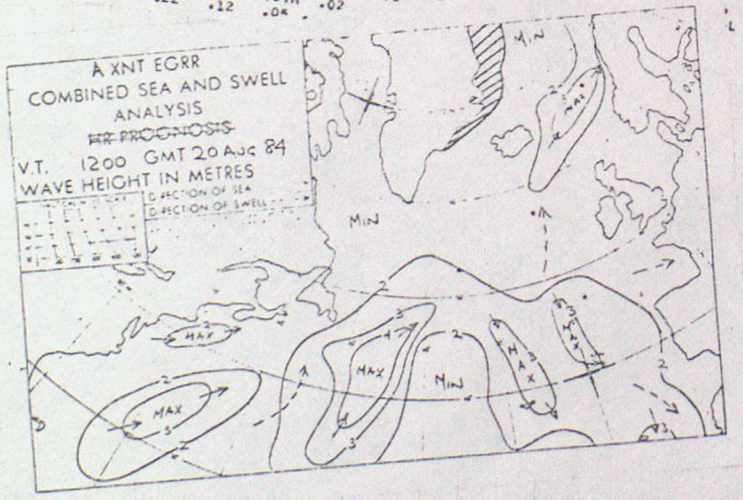

SHIP ROUTEING

OFFSHORE OPERATIONS

GRID CODE

```
444 10000 20000 30028 40114 53047 60075
555 74304 10102 666
 87697
G00000 F000 110000
GRID 74304 10202
111 10005 20000 68308 71100 81036
337
24 041704180417041804180519051904210522042302250226022602270128
C228022802270130023201320133013401350236023601010136003301340033
****
25 041704190417041804180520062105220232023022402260225022601270128
012801290130013201340132013601360202020302010236023400260*******
****
26 021804190419052004200521042204220232023022402260225022601260131013201330
012901300231023302360202010202020202020202010236013400300*******
****
27 032004200421042104210322032203210225022602260226012601270202010301350
013101310234023602020201020102020202020202010236013400300*******
****
28 032103210322042104230423032202240226022602260127020201030135
013302330236020102020101010003400340136023501340133013131*******
****
```

WAVE AND SURGE MODEL GRID AREAS

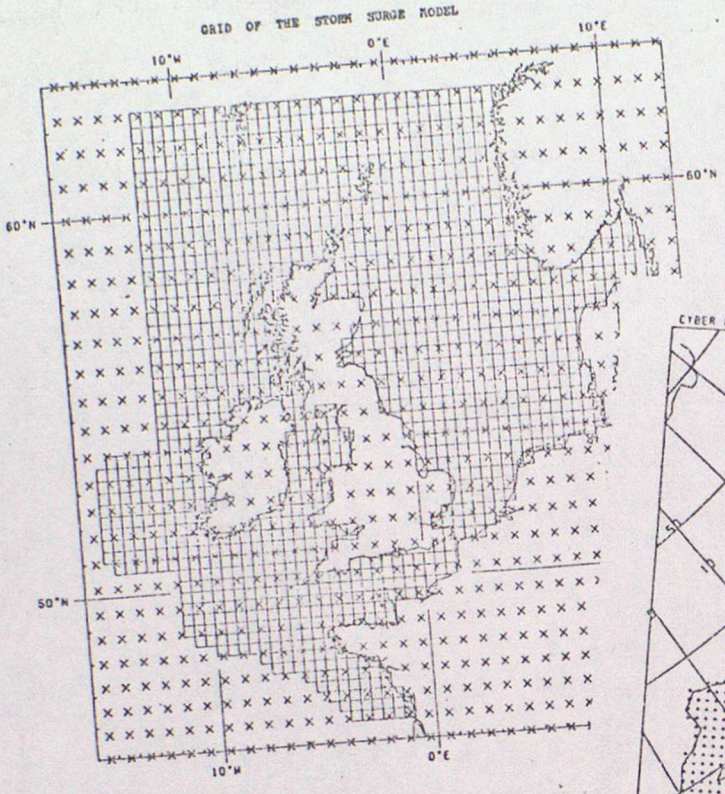

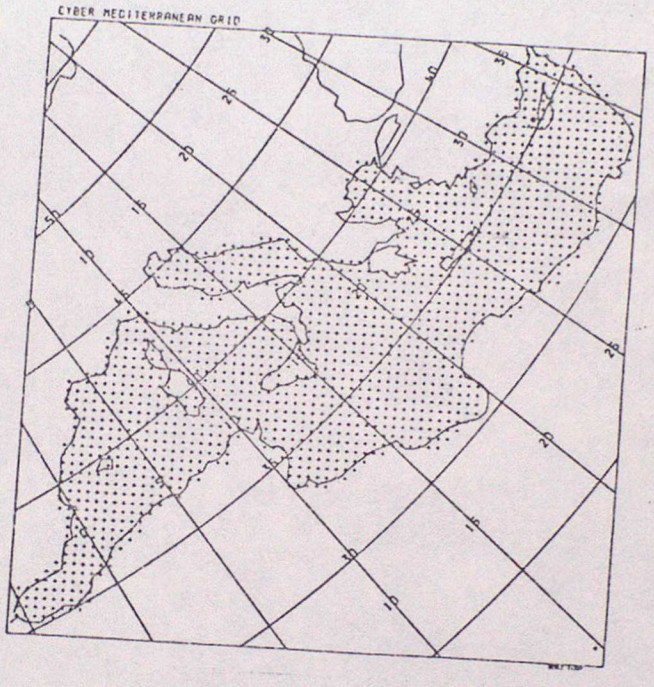

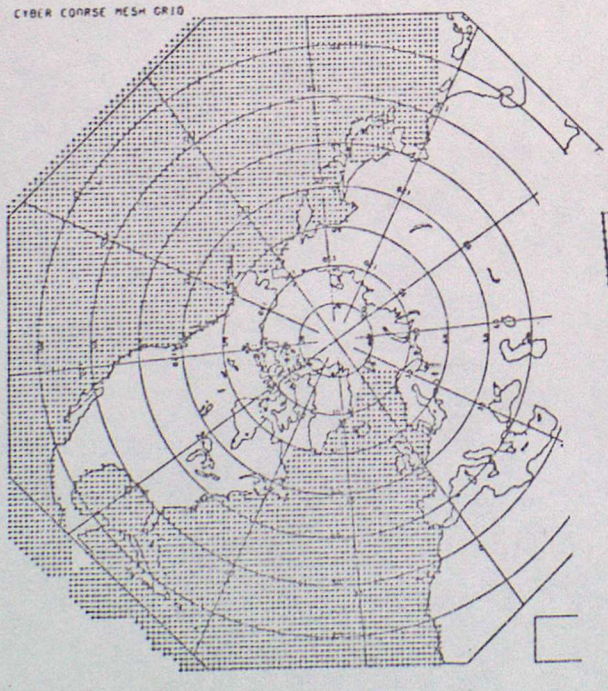

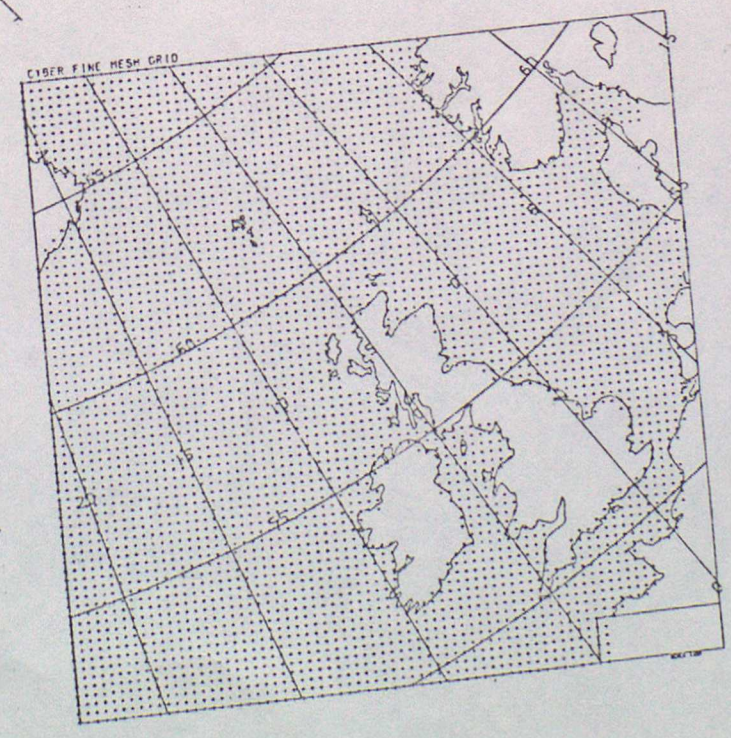

ADVANCED LECTURES 1985

OPERATIONAL NUMERICAL WEATHER PREDICTION

Lecture 9

Verification results

A. P. Day

OBJECTIVE VERIFICATION OF NUMERICAL FORECASTS

Introduction

Verification involves the measurement of the accuracy of forecasts. This is usually achieved by calculating differences between forecast quantities and estimates of the true values of those quantities at a large number of points distributed in space and/or time. Verification statistics are often used to summarise the differences. For example, using forecast fields from a numerical model, valid at some given time, verification statistics may be used to summarise the set of differences between the forecast and the observations (at the observation positions) or between the forecast and the objective analysis (usually at the gridpoints, though in this case also there may be reasons for carrying out the verification at the observation positions).

Verification Statistics

In the Meteorological Office the forecast error statistics used most commonly are the root mean square error, the mean error and the correlation coefficient between forecast and actual changes (known as the tendency correlation).

In addition, two types of statistic are calculated to assist in the interpretation of forecast error statistics. The variances of the forecasts and of the observations (both evaluated at the observation positions) are useful in assessing whether the forecasts have a realistic character, or whether they are, for example, too smooth. Statistics for persistence forecasts are useful in assessing the effects of atmospheric changeability on the forecast error statistics, so that statistics from different periods can be more readily compared.

Statistics are calculated for a wide range of forecast fields at different levels in the atmosphere, for various geographical areas and for various forecast periods.

Verification statistics may be displayed in tabular form or as time series plots. In addition, maps are produced which show the geographical distribution of error statistics for a set of forecasts.

Uses of verification results

The various statistics are used for the following purposes.

(i) Monitoring changes (short-term and long-term) in the performance of a numerical prediction system.

(ii) Comparing the performance of different numerical prediction systems.

(iii) Testing the impact of proposed changes in formulation or procedure.

(iv) Diagnosing systematic errors in model behaviour as a basis for further research.

Limitations

One of the main problems in objective verification is the choice of an estimate of the true state of the atmosphere. Obviously, the observations provide one such estimate, and one of the routine verification schemes used in the Office verifies forecasts against sets of relevant observations from the Synoptic Data Bank. Since observations are not perfect, a simple quality control procedure is applied before the observations are used. Another problem with verification against observations is the irregular distribution of the observations. For example, verification against radiosonde data is heavily biassed to continental regions, and this may hinder the proper interpretation of verification results.

The operational objective analyses provide another estimate of the true state of the atmosphere. Objective analyses also have errors. For example, a human analyst may well be able to recognise the validity of an extreme observation, but the objective analysis is likely to underfit it. Also, different objective analysis systems have different errors, often influenced by the prediction model which provides first-guess fields or performs the data assimilation. In the Office, verification against objective analyses is performed at several levels and over the entire globe. In addition, sea level pressure forecasts for a small region near the UK are verified using the subjective surface analyses prepared in the Central Forecasting Office. Though limited in scope, this verification against subjective analyses is perhaps the most satisfactory for monitoring long-term changes in performance.

There are also limitations when it comes to interpreting the implications of verification statistics. For example, a numerical forecast which successfully simulates the genesis of a new depression, but with a small positional error, may score a higher root mean square error than another forecast which missed the new system altogether. Or again, a pair of forecasts with very similar root mean square errors for sea level pressure may (in certain synoptic situations) imply significantly different air flows and surface temperatures at particular locations. These considerations show the need for verification systems that are tailored to particular applications of forecasts, but these are beyond the scope of the work described here.

Wherever possible, objective verification statistics are supplemented by subjective comparison of charts when assessing proposed changes in numerical models.

Examples

1. Intercomparison of models

Figure 1 demonstrates how, when verified against a common independent data set, verification statistics can be used to compare the results from different forecast models. Operationally, forecasts received from ECMWF and NMC, Washington, are both verified against the same observations as the 15 level model.

2. Use of persistence statistics to help interpretation

Figure 2 is an example of the use of persistence forecasts in monitoring the effect of a change to the forecast model. A change to the forecast model in December 1984 included a gravity wave drag parametrisation that reduced the root mean square errors of sea level pressure compared with the earlier version of the model. The monthly mean errors plotted in the diagram showed a characteristic variation with the persistence error for each month before December. However changeable a month, measured by the persistence errors, one might expect the earlier version of the model to give forecast errors lying between the two continuous lines. The plot labelled Dec* shows the error for the month following the change in the forecast model and indicates a reduced forecast error compared with the earlier months when normalised by the persistence errors.

3. Diagnosis of systematic errors

Figure 3 shows some output from the error map subroutines of the operational verification programs. The map enables the systematic model errors to be located geographically. The diagram below this illustrates the zonal component of the monthly mean error for the three winter months of 1983-4 and for January 1985. This latter month was the first calendar month following the major change to the 15 level model in December 1984 (inclusion of a gravity wave drag parametrisation).

In this diagram the mean error is split into four latitude bands of the northern hemisphere, the mid points of which appear on the left side of the diagram. Each horizontal line represents 0.5 mb of the difference between the mean error in adjacent latitude bands, thus the smaller the spacing between these lines the greater is the zonal error between the two adjacent latitude bands. The total difference across all four latitude bands is given along the top of the diagram. This diagram illustrates in a simple way the characteristic of the 15-level model of 'increasing the westerlies' in these latitudes. One of the reasons for the change to the model in December 1984 was to try to reduce this type of error.

4. Seasonal and latitudinal variation of errors

Figure 4 demonstrates the seasonal and latitudinal variation in mean error of sea level pressure. It can be seen that the calculated errors in the extratropical northern hemisphere are of a different sign to those in the extratropical southern hemisphere. However, this may be partly due to the different distribution of observations in the two hemispheres.

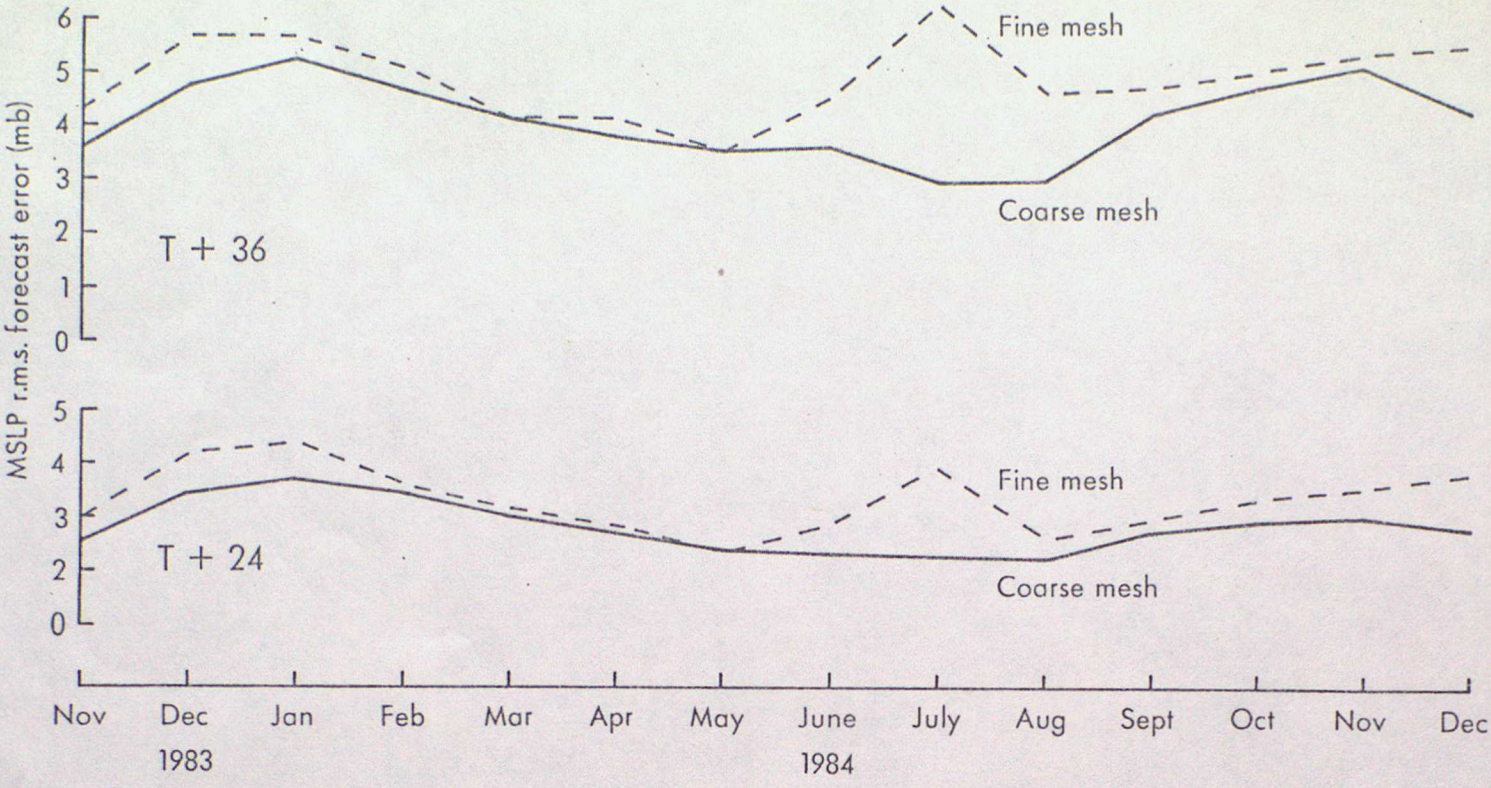

Fig. 1 A comparison of the two operational versions of the 15-level model. Verification against the same set of observations in an area including the UK and parts of western Europe.

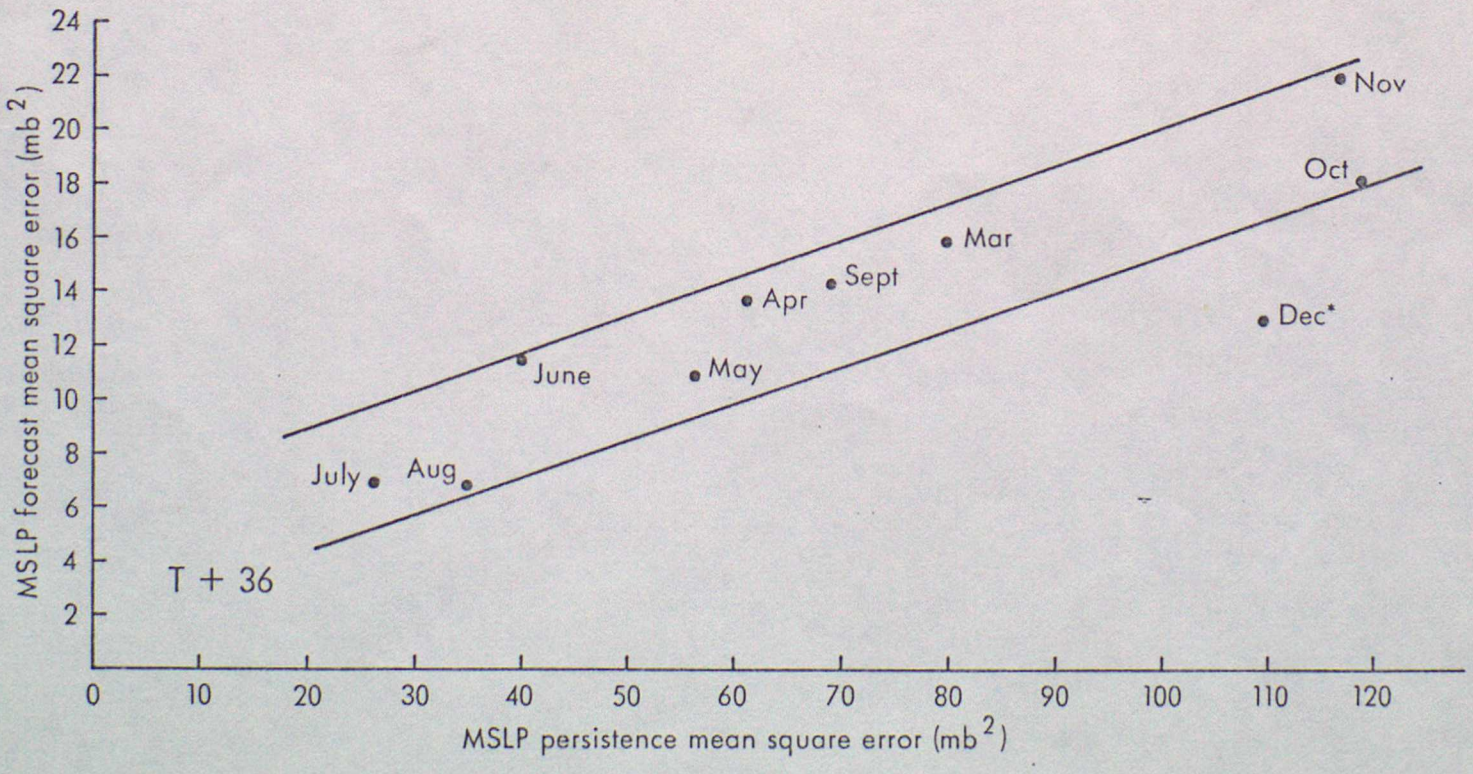

Fig. 2 This shows the variation in performance of the coarse mesh model with the changeability of the atmosphere. Verification against observations in the same area as for Fig. 1.

Mean forecast error (T + 72) for January 1984 at 500 mb. Height in decametres.

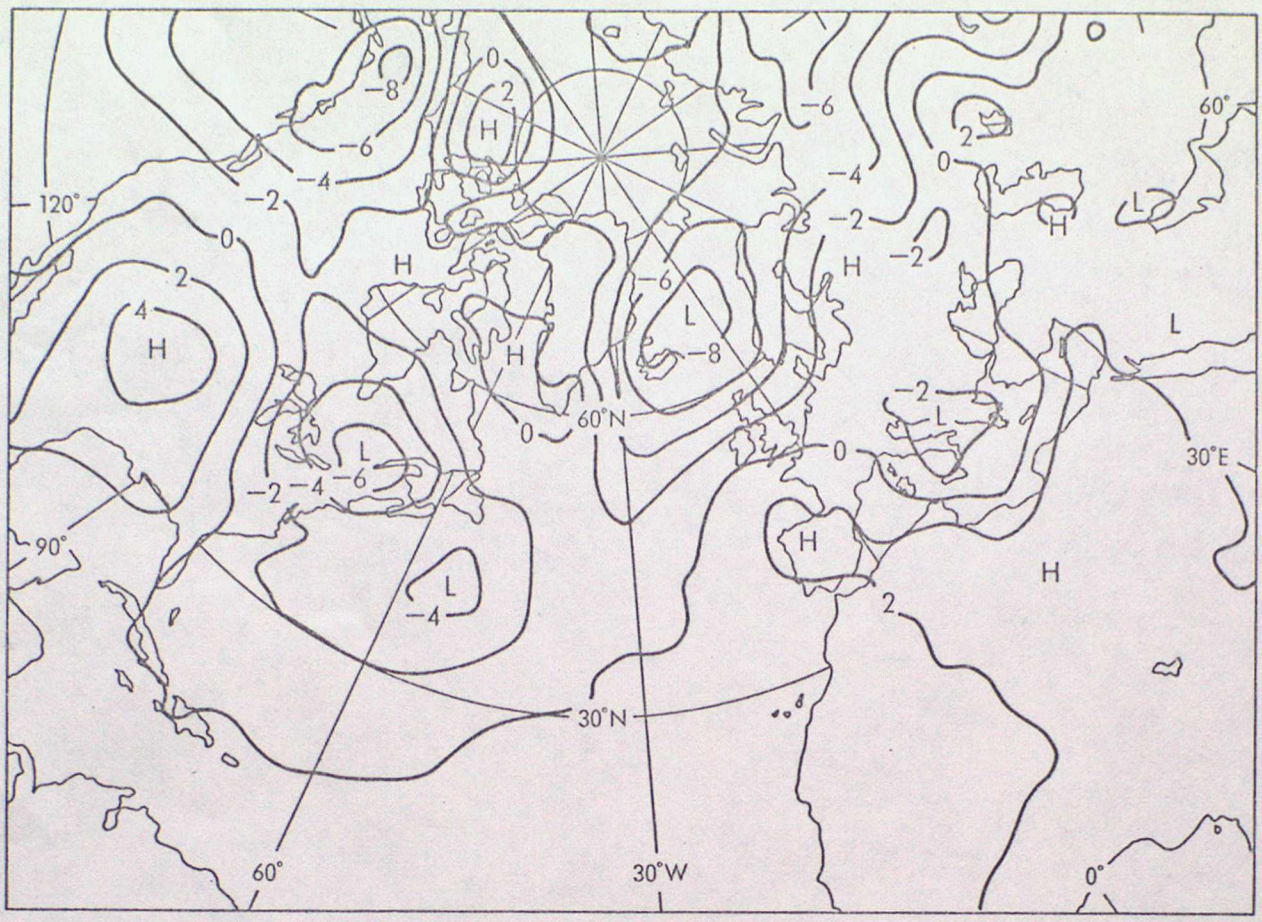

Zonal component of mean forecast error, MSLP, T + 120

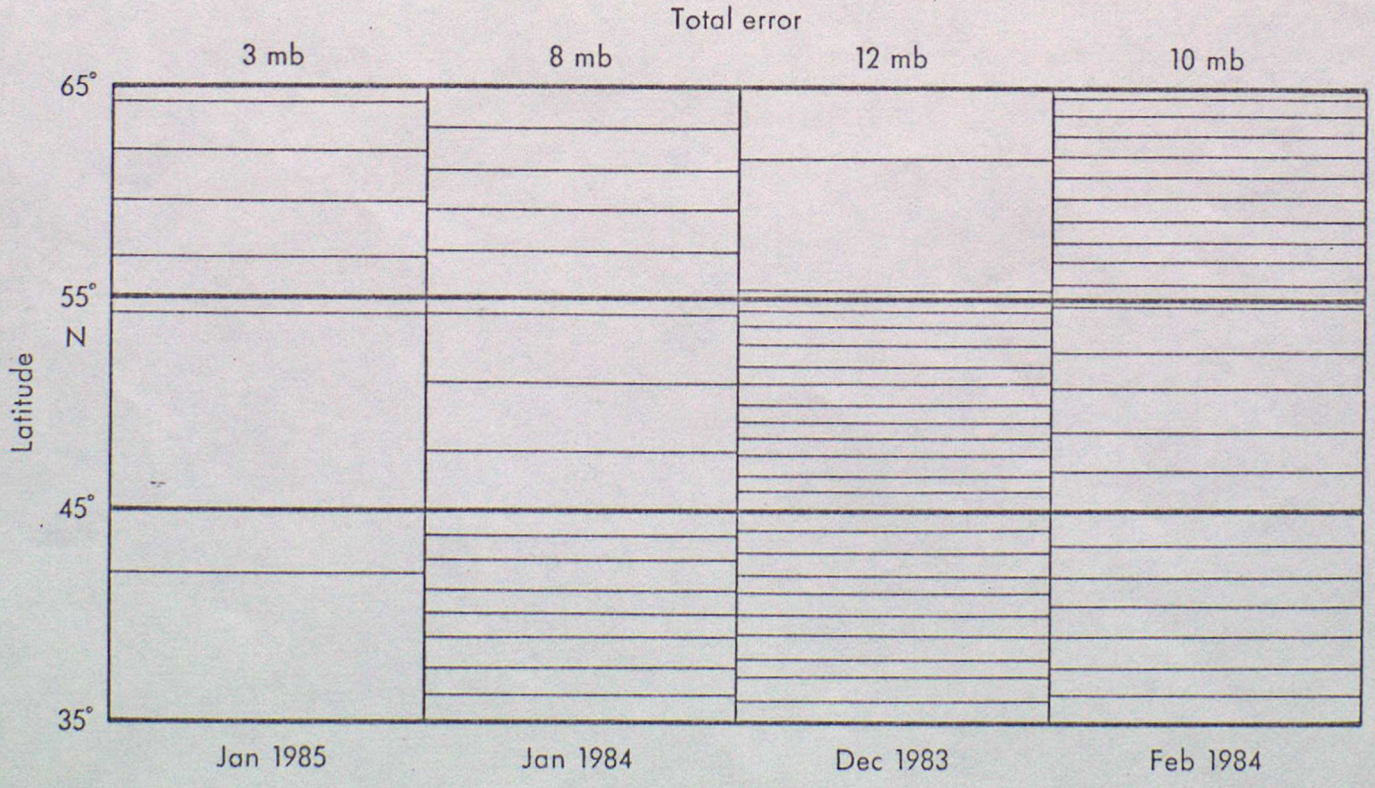

Fig. 3 Two ways of representing the systematic errors in numerical models. (See text for an explanation of the diagrams).

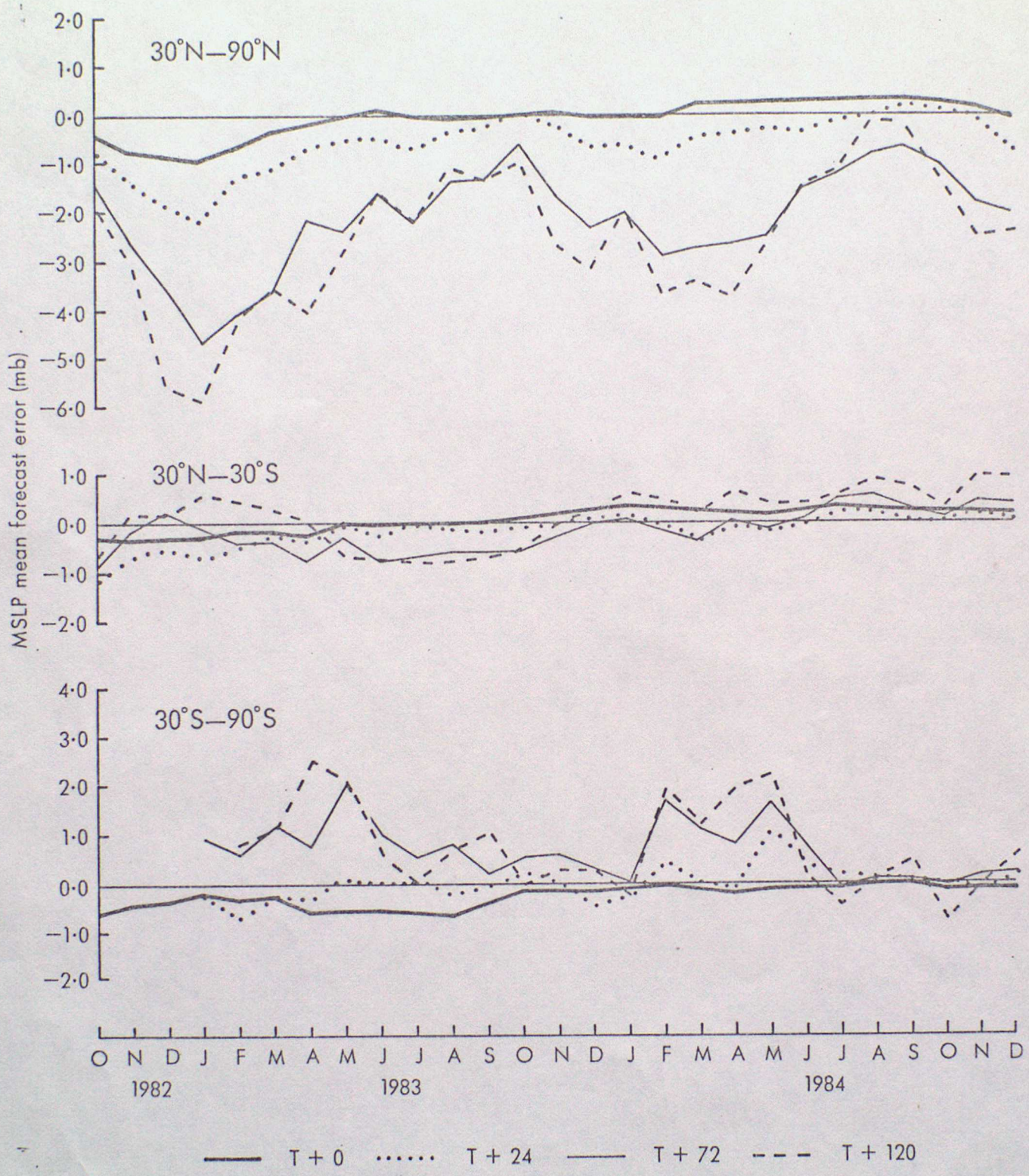

Fig. 4 Time series of monthly mean forecast error of the sea level pressure field. The three graphs are for the northern hemisphere north of 30° (top); the tropical area 30°N—30°S (centre) and the southern hemisphere south of 30° (bottom). Verification against observations.